OPTIMIZATION OF COIL GEOMETRIES FOR ELECTROMAGNETIC INDUCTION SENSORS

by
Mehmet Ali YEŞİL

Submitted to the Institute of Graduate Studies in
Science and Engineering in partial fulfillment of
the requirements for the degree of Master of Science
in
Electrical and Electronics Engineering

Yeditepe University

2014

OPTIMIZATION OF COIL GEOMETRIES FOR ELECTROMAGNETIC INDUCTION SENSORS

APPROVED BY:

Assoc. Prof. Dr. Korkut Yeğin .....
(Supervisor)

Prof. Dr. Canbolat Uçak .....

Instructor. Deniz Pazarcı .....

DATE OF APPROVAL: …./…./….

ACKNOWLEDGEMENT

I would like to express my sincere gratitude to my advisor Prof. Korkut YEĞİN for continuous support during my master thesis and for his patience, motivation, enthusiasm, extensive knowledge, and especially for his encouragement. His guidance helped me in research and writing of this thesis.

Besides my advisor, I would like to thank to The Scientific and Technological Research Council of Turkey (TÜBİTAK) for supporting my master program by offering a scholarship for 2 years.

ABSTRACT

OPTIMIZATION OF COIL GEOMETRIES FOR ELECTROMAGNETIC INDUCTON SENSORS

In this thesis, several coil geometries for electromagnetic induction sensors are designed and optimized to provide good performance at desired frequency using FEKO electromagnetic simulation program. After that, a comparison of different coil geometries was performed. Studied coil geometries are DD-type coil, coaxial type coil, and 8-shaped coil. Also, their performances were evaluated in detection of canonical, nonmagnetic metallic targets such as small sphere, coin, and small nail. After optimizing the coil geometries in free space, effects of several soil types, where targets lie beneath earth surface, with different electromagnetic characteristics such as dry soil, wet soil and highly mineralized ferrous soil were investigated for detection of these canonical objects. Induced current in the receive coil was simulated and observed for all types of coil geometries and soils at certain depths in order to characterize detection capabilities. Also, a prototype was prepared for coaxial type coil and induced voltage measurements were performed on air in the presence of different targets.

ÖZET

ELEKTROMAGNETİK İNDÜKSİYON SENSÖRLERİ İÇİN BOBİN GEOMETRİLERİ OPTİMİZASYONU

Bu tezde FEKO elektromagnetik benzetim program kullanılarak, elektromagnetik indüksiyon sensörleri için çeşitli geometrilerde bobin türleri tasarlandı ve istenilen frekansta iyi performans göstermeleri için en uyun hale getirildi. Temel olarak DD tipi bobin, ortak eksenli tip bobin ve "8" şekilli tip bobinler üzerinde çalışıldı. Ayrıca, tasarlanan bobinlerin performansları küçük bir küre, bozuk para ve bir çivi olmak üzere farklı geometrilerdeki üç farklı metalik hedefin tespitinde incelendi. Bobin geometrilerini serbest hava ortamında optimize ettikten sonra, hedef cismin altında bulunduğu farklı elektromagnetik özelliklere sahip toprak türlerinin bobinlerin performanslarına etkileri değerlendirildi. Bu toprak türleri sırasıyla kuru toprak, ıslak toprak ve yüksek oranda mineral içeren topraktır. Tüm toprak türleri ve bobin geometrileri için alıcı bobindeki indüklenen akım değerleri belirli derinliklerde benzetilerek bobinlerin tespit yetenekleri karakterize edilmiştir. Ayrıca ortak eksenli bobin tipi için serbest hava ortamında farklı metal hedeflerle indüksiyon voltajı ölçümleri gerçekleştirildi.

TABLE OF CONTENTS

LIST OF FIGURES

LIST OF TABLES

LIST OF SYMBOLS / ABBREVIATIONS

MD	Metal Detector
VLF	Very Low Frequency
PI	Pulse Induction
BFO	Beat-Frequency Oscillation
CW	Continuous Wave
DC	Direct Current
AC	Alternating Current
EM	Electro-Magnetic
E	Electric Field
B	Magnetic Field
EMF	Electro-Magnetic Force
nA	Nano Amper
μA	Micro Amper
mA	Mili Amper
MoM	Method of Moments
PEC	Perfect Electric Conductor
S	Siemens
Ω	Ohm
OpAmp	Operational Amplifier
V	Volt
μH	Micro Henry
F	Farad
V_{pp}	Peak to peak voltage

1. INTRODUCTION

Metal detectors are portable electronic devices that are widely used in humanitarian demining, military applications, coin shooting etc. Basic aim is detect a target such as mines, valuable coins, jewelry or specific buried objects that are placed underground when using metal detectors. Their importance and usage are significantly increasing in all industrial areas and in daily life during last century. Performance of any type of metal detector depends on a set of variables including target properties, soil properties and coil properties itself. So, lots of research projects and academic studies about them have been performed in universities, research centers etc. In this thesis different coil configurations and effect of different soil types are investigated. It is performed that the possibility of detecting and distinguishing between different targets based on both their characteristics and soil electromagnetic conditions.

There are some studies about coil configurations by designing their coil circuit models for VLF metal detectors that operate below MHz range [1]. Another study about coil design and a comprehensive research of soil effect for spherical targets is [2] but for PI metal detectors this time. This paper presents the effect of different excitation signals for metal detection and discrimination [3]. Issues on performance evaluation and comparison of metal detectors in terms of their detection capabilities are studied in [4]. The main effort in metal detectors studies is focused on soil electromagnetic properties. Soil interference of especially highly mineralized and magnetic soils is deeply investigated in this report [5]. Another study for relating soil properties to performance of metal detectors by modeling direct and indirect soil parameters and also variation of these parameters with space and time which have great effects on metal detectors is presented in this paper [6]. Other useful studies about the properties of soil that surrounds the targets are [7], [8] and [9].

Another study, [10] gives an idea about localization and detection of buried objects in diverse soils using computer aided approaches by modeling soil EM characteristics for a well-defined area. Also, there is a research about multi-channel transmit/receive metal detector coil design for vehicular applications that can be found in [11].

1.1 A BRIEF HISTORY OF METAL DETECTORS

From the beginning of 20th century many scientist and engineer were attempting to invent an instrument that could pinpoint any metal in a specified area using electromagnetic induction principles to facilitate the determination of ore-bearing rocks for miners. Legacy machines were inefficient, unstable, using a lot of battery power and working for very limited depths. Alexander Graham Bell had some studies over them but first modern, useful detectors appeared in the beginning of 1920s by Gerhard Fisher. Dramatic growth in their investigation occurred in World War II. A Polish lieutenant, Józef Stanislaw Kosacki invented Polish Mine Detector which was a metal detector allocated from its legacies for its new coil design. It actually consist of two coils; transmit one is directly connected to an oscillator and receive one is connected to an amplifier and to a headphone. Referring this design, Polish Mine Detector can be considered as the basis of modern metal detectors.

Importance and usage of the metal detectors are significantly increased during last century in demining of demilitarized zones from landmines after wars or conflicts. Mines began to appear on a large scale during World War I, as an answer to another new piece of weaponry; the assault tanks. Germans improved the damage properties of landmines using new techniques in their production in order to combat to tanks. Especially in World War II and in the lots of civil wars millions of anti-personnel or anti-tank mines were laid. After that wars ended, those mines were abandoned to their fates without doing any study for demining them. And the worst thing about landmines is that nobody knows where exactly they are since they were laid indiscriminately during war years. In these days, it is estimated that each day over 70 people are killed or injured by anti-personnel mines. Landmines also injure or kill hundreds of thousands of animals every year. So, detecting and demining them has become a very important issue in the last twenty years.

As it is cited above, metal detectors are not only used for demining operations but also commonly used in coin shooting applications. By choosing an appropriate metal detector and by considering the properties of target, characteristics of search medium and required sensitivity, specific material concealed underground can be easily detected and identified. Also, many archeologists use MDs in historical excavations to find antique coins or similar items. One of other major deployment of MDs is as security detectors. A security metal

detector is an electronic device that alerts in case of unwanted or suspicious metal objects pass within range of the device. There are many different types of metal detectors such as from walk-through models, hand-held wands etc. Some systems combine more than one type of detector. Security metal detectors are usually placed at entrances of government buildings, shopping malls, airports and anywhere that screening for guns or dangerous metallic materials. They have become very common and mandatory after a couple hijacking series in United States during 1970s. Moreover certain types of MDs are being used as industrial metal detectors in the areas of textile, food, beverage, chemicals etc. as a kind of sensor. For example in food industry, canned food producers use industrial type of metal detectors in order to detect metal shards from broken machinery parts or from can itself and prevent them from contaminating in the food. In industrial metal detectors generally coaxial coil arrangements are used to be able to detect little metallic parts smaller than 1mm in length. In the following figure some types of commercial hand-held and fixed metal detectors that are deployed for different applications.

Figure 1.1. Examples of different types of metal detectors

1.2. TYPES OF METAL DETECTORS

In the market, anyone can see different types of metal detectors work in various different ways, but the theory behind all types of metal detectors is quite related to each other. Also, their usage is very simple and similar. Simply, a metal detector consists of a search head and a handle, and as we sweep that head back and forth over the ground, detector scans the whole ground beneath our feet. When it is passed over a target object, an audible signal that is amplified by electronic circuit of the detector occurs. In recent years some advanced metal detectors began to display the type of metal that detected and how deep it locates in the ground. Any type of metal detector head contains a coil or couples of coils that are used as transmitter and receiver coils. Electromagnetic induction properties of coils are used for detecting and these coils can be considered as inductors operating at relatively low frequencies.

Metal detectors can be categorized in three major types;

- Very Low Frequency (VLF) or Induction Balance (IB) Metal Detectors
- Pulse Induction (PI) Metal Detectors
- Beat-Frequency Oscillation (BFO) Metal Detectors

There are basic differences in the working principles of these metal detectors but, operation of them is very similar and quite simple.

1.2.1. Very Low Frequency (VLF) Metal Detectors

In this type of MDs, detector includes minimum two coils inside its search head. Number of transmit and receive coils can be more than one depending on coil arrangements used. Inside the metal detector's loop there is a coil of wire called the transmit coil. If a current passes through such a coil it will generate a field as shown in Figure 1.1. If we pass direct current (DC), it will generate a static magnetic field, but if we pass alternating current (AC), then it will generate an alternating magnetic field. In the operation of metal detectors, we will be interested in AC. When we bring a second coil close to the first one,

the signal from the first coil will couple into the second coil and an induction voltage and current will occur on the second coil via induction.

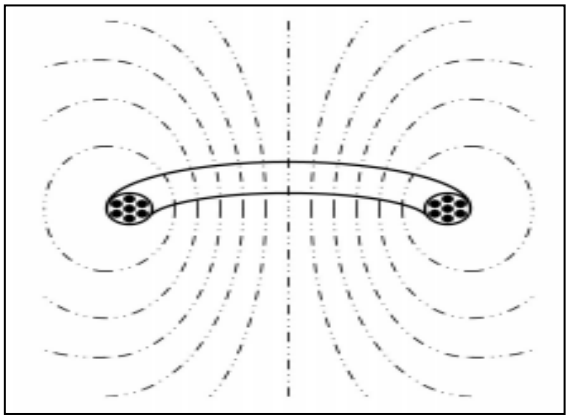

Figure 1.2. Magnetic field lines produced by a current carrying coil [12]

Also, when the current flows in a given direction, a magnetic field is produced either into the ground or out-of-ground depending on direction of current in the transmitter. Any electrically conductive target object under the ground will have a circular flow of current induced named as eddy currents inside of it by the influence of the changing magnetic field produced by transmitter alternating current. After that, this current flow on the surface of the conductive target object will produce its own reverse (in the opposite polarity of transmitter magnetic field) changing magnetic field, in turn. This effect is illustrated in Figure 1.3. This changing reverse magnetic field also triggers a current in the receive coil. However, as transmit coil produces a huge magnetic field over receive coil, reverse magnetic field caused by metallic target will be relatively small, very difficult to distinguish from transmitter coil effect. In order to surmount this problem the receive coil needs to be arranged in such a way so that nearly all of the current flows in it due to the influence of the transmitted field is cancelled out. Therefore, the reverse magnetic field produced by the currents flowing in the metallic target object will cause significantly detectable currents to flow in the receive coil that can be amplified by the electronic circuitry of the detector. In other words, different types of received and transmit coils arrangements need to be studied in order to find a way to prevent currents on receiver coil produced by metallic object on being swamped in the presence of currents resulting from the much stronger transmitter field.

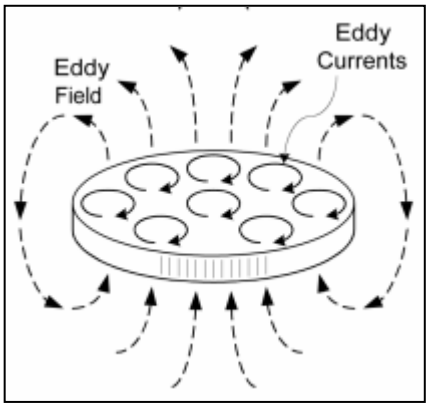

Figure 1.3. Illustration of Eddy Currents and Eddy Fields on metallic target [12]

The resulting received signal produced by metallic target will usually appear delayed when compared to the transmitted signal. This delay can be explained with the tendency of conductors to impede the flow of current and to impede changes in the flow of current. It is a well-known effect named as phase shift. As metallic target object becomes larger, thicker, phase shift will become larger. Also objects made from excellent conductors such as gold, silver, copper etc. will cause a larger phase shift since they are primarily inductive. However, smaller objects and targets made from relatively low conductance materials will cause a smaller phase shifts as well as they are primarily resistive materials.

Another important point when demystifying VLF metal detectors is behavior of the ferromagnetic materials such as nickel, cobalt, iron and their alloys that conduct current poorly but cause a strong magnetic field by being magnetized that will be picked up by the receiver and may cause a false alarm. So, anyone in coil design study need to consider this effect because most types of soils and sands contain small grains of iron-bearing minerals which can cause them to appear largely ferromagnetic to the detector.

Related with the conductivity and magnetic properties of the medium, different soil types may perform different characteristics in the running of metal detectors but this topic will be discussed in the subsequent chapters.

1.2.2 Pulse Induction (PI) Metal Detectors

Another type of metal detector that is less common used in these days is Pulse Induction metal detectors. In PI type of metal detectors, search head may include a single coil that can work as both transmitter and receiver or may have two or more coils working together that differs from the VLF type metal detectors. In this technology basically MD sends very powerful but relatively short pulse signals of current through a coil of wire. Every pulse generated by the metal detector creates a magnetic field towards ground. When the pulse ends, the magnetic field reverses its polarity and collapses suddenly, resulting in a sharp electrical spike that is called as reflected pulse. After a cycle of sending pulse and creation of reflected pulse, another pulse is then sent and the whole process repeats cyclically. Generally PI type MDs send about 75-1000 pulses per second depending on its model and its purpose of use.

Theory of PI MDs differs from the theory of VLF MDs in the method of detection. When the search head of a PI metal detector is over a metal object, the pulse creates an opposite magnetic field in the object just like in VLF MDs, since a metal object that is under influence of an electro-magnetic field interacts with this field due to self-induction of itself. So, after end of the transmitted electro-magnetic pulse, a secondary fading electro-magnetic field is transmitted from the object**.**

But, when the magnetic field of pulse that is created by transmitter coil collapses with time causing the reflected pulse, the opposite magnetic field of target makes it last much longer for the reflected pulse to completely disappear. This phenomenon can be likened to effect of reflection sound named as echoes. In a PI metal detector, the magnetic fields from target objects add their echo to the reflected pulse, making it last a fraction longer than it would without them. Coil voltage waveforms of PI metal detectors in operation can be seen in Figure 1.4.

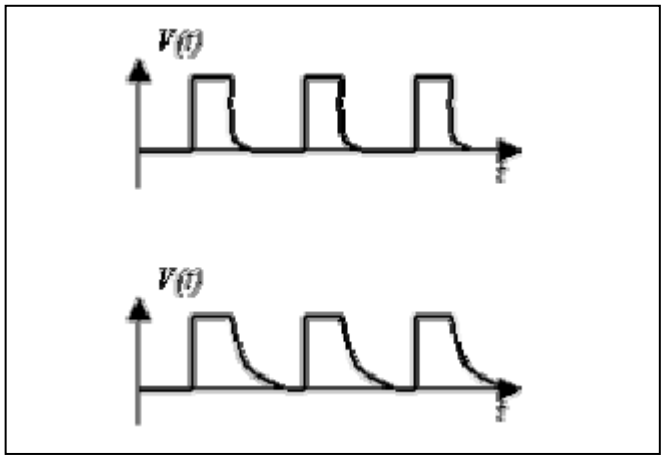

Figure 1.4. Coil voltage waveform of the pulsed induction metal detector without presence of any metallic object (upper) and with presence of a metallic object (lower) [9].

Electronic circuit part of the metal detector simply compares the length of expected reflected pulse and actual reflected pulse, so it can decide if any target underground has made the reflected pulse disappear later than expected by producing an opposite magnetic field. Thus, this latency effect will give the information if a metal object is present in the proximity of our metal detector. In the circuit part of PI metal detector, use of integrator is necessary in order to receive signal, amplify it and convert that signal to a DC signal. And this DC signal is used to create an audible signal via an audio circuit and speakers in case of detection of any metallic target. A simple block diagram of PI type metal detectors is shown in Figure 1.5.

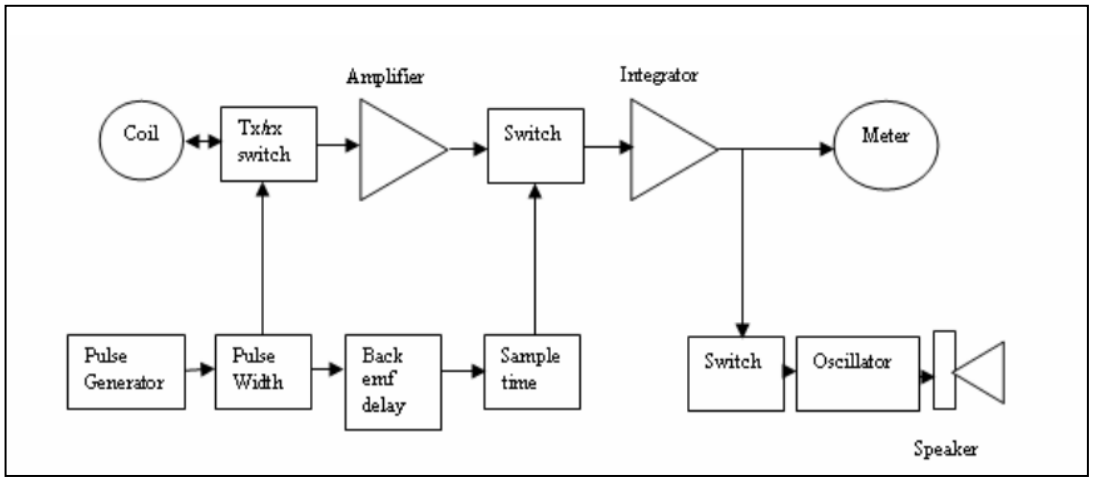

Figure 1.5. Block diagram of PI metal detectors

PI metal detectors have an advantage when dealing with certain types of soil that are relatively conductive and they also offer huge depth penetration of the electro-magnetic pulse thanks to allowing a design of huge searching coil. Moreover, PI type metal detectors are less sensitive to climate and temperature effects than other types of metal detectors. On the other hand they have difficulty in the separation of different types of targets.

1.2.3 Beat-Frequency Oscillation (BFO) Metal Detectors

Beat frequency oscillator (BFO) type metal detectors are the simplest and oldest type of metal detectors. Their simplicity comes from the ease and low-cost of their construction. However, they are less sensitive to detection and also offer less accurate performance compared to other types of metal detectors. In a BFO type metal detector, there are two coils, large one is used in the search head, and a smaller one is located inside the control box. Also, the basic beat-frequency metal detector includes two oscillators which are tuned to operate near the same frequency. In other words search head coil oscillator and reference oscillator which is located inside the control bow of the detector, of a BFO type metal detector operates at frequencies separated by only a few 100 Hzs. So, the frequency of these pulses is slightly offset between the two coils.

With the aid of a mixer these two near frequency signals are mixed to produce both difference and sum of two different frequencies. Then this mixed signal is made pass over

low-pass filter to remove unwanted harmonics. Thus, a BFO type metal detector works by comparing two different frequency oscillators in order to detect metal targets.
When there is no target beneath detector, the coil with an inductance held constant is called the reference coil and the coil that detects metal has nearly equal inductance.

When we pass the search head of detector over any metal object, the inductance of the search head changes due to presence of a detected object by causing a frequency deviation depending on location, size and material of object in the oscillating circuit. This small deviation in the frequency will cause a signal that alerts the user [15]. A basic representation of working principle of a BFO type metal detector is illustrated in the following figure.

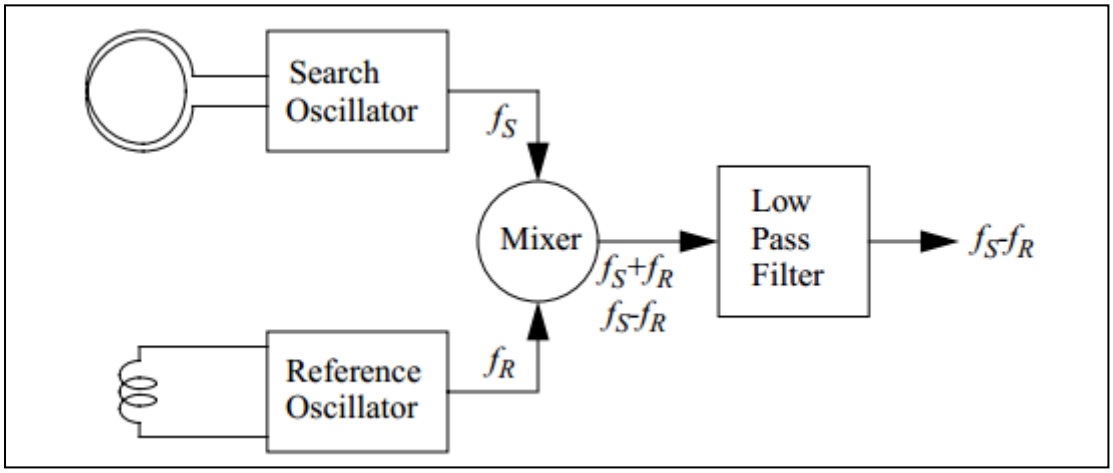

Figure 1.6. Basic BFO type metal detector [14]

2. MAGNETIC INDUCTION

In this part of thesis the theory behind VLF type metal detectors and some theoretical calculations will be covered.

Maxwell's equations are the fundamental laws of electromagnetism and necessary to explain working principles of metal detectors by demystifying relation between various electromagnetic (EM) fields.

Maxwell's four equations are formulated below;

$$\nabla x E = -\frac{\partial B}{\partial t} \quad (2.1)$$

$$\nabla x H = J + \frac{\partial D}{\partial t} \quad (2.2)$$

$$J = \sigma E \quad (2.3)$$

$$B = \mu_0 \mu_r H \quad (2.4)$$

Equation 2.1 basically describes the connection between an electric field E and the equivalent magnetic field B in a given certain point. In order to relate it with electromagnetic induction, it can be rearranged as in Equation 2.5 in the integral form by using Faraday's Law of Induction which denotes how a magnetic field will interact with an electric circuit to produce an electromotive force (EMF) called as electromagnetic induction.

$$\oint_C E \,.\, dl = - \frac{\partial}{\partial t} \oint_S B.dS \quad (2.5)$$

It states that the induced electromotive voltage in a closed loop equals the time rate of change of the magnetic field through its surface.
Equation 2.2 describes the connection between the magnetic field strength and current density J added with the displacement current, where H represents the magnetic field strength and D represents electric field strength. This equation is also very important since it gives the relation between magnetic field and the associated current in a conducting wire and can be useful to understand from where Biot-Savart law comes out.

Equation 2.3 describes the connection between conductivity of the material with electric field created on the object and Equation 2.4 explains relation between magnetic properties of materials with their magnetic field. All of these mathematical derivations have a significant importance in order to understand operation of detector’s coils.

2.1. BASIC PRINCIPLE OF DETECTOR HEAD

In this part of thesis it is going to be described the working principle of search head part of metal detectors in a more detailed way. In the following figure, two transmit coils will be represented as Tx1 and Tx2, one receive coil, will be represented as Rx can be seen.

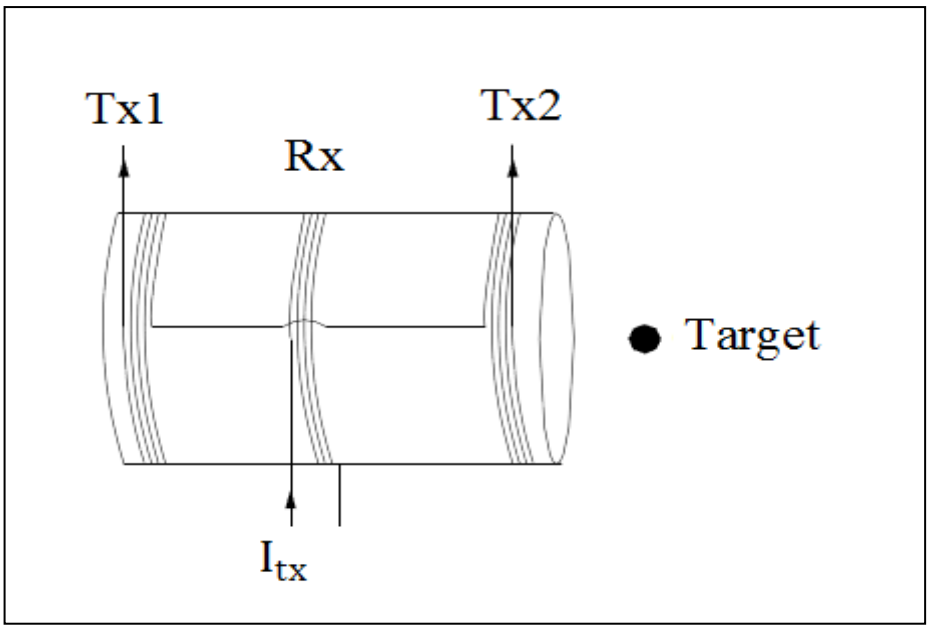

Figure 2.1. Illustration of detector search head consisting of two transmitting coil Tx1, Tx2 and one receiving coil Rx.

In the figure above two transmit and one receive coils are placed in a specific proximity where magnetic field produced by Tx1 and Tx2 will be canceled out on Rx coil and so it will be balanced in order to work properly when detecting a metal target.

In transmit coils a sinusoidal time dependent current $I_{tx}(t) = \sin w_0\, t$ is applied to produce a magnetic field which propagates towards the metallic target and in other directions as well. Consequently, generated magnetic field by source current can be expressed via Biot-Savart law as;

$$B_{tx}(t) = \frac{\mu_0\, I_{tx}(t)}{4\,\pi} \int_0^{2\pi} \frac{dl\; x\; \vec{r}}{r^3} \tag{2.6}$$

Where

- μ_0 is a constant and represents magnetic permeability of free space
- $I_{tx}(t)$ is the current in transmit coils
- dl is an infinite small length vector where integral will be calculated
- $\vec{r}$ is the vector represents distance from coil to point of calculation.

Also $B_{tx}(t)$ can be calculated by using inductance formulas as follows,

$$B_{tx}(t) = \frac{N_{tx}\,\mu_0\,I_{tx}}{2\,R_{tx}} \tag{2.7}$$

Where

- N_{tx} is number of turns of transmitting coils
- R_{tx} is radius of transmitting coils.

Then, this magnetic field will produce an electromotive force (emf) in receiving coil(s) that can be calculated by Faraday's Law of Induction as,

$$\varepsilon = N_{rx} \oint_C E_r \,.\, dl \tag{2.8}$$

Where

- N_{rx} is number of turns of receiver coil
- E_r is electric field in the receiver coil
- dl is an infinite small length vector where integral will be calculated

And this emf can be rewritten in terms of magnetic field produced by transmitter coil(s) as follows. Negative sign in the right hand side of the equation will be appear due to Lenz's Law.

$$\varepsilon = -N_{rx}.\frac{\partial}{\partial t}\int_S B_{tx}\,.dS \tag{2.9}$$

If we apply all of these calculations above by taking into account two transmit coils, the resulting emf force in the receive coil will be nearly zero and it will be called balanced provided that dimensions of transmit coils are equal and they are placed at equal distances from receiver coil. This situation can be reversed by using two received coils and one transmit coil and placing them similarly to the case described above. In other words, different types of structures and different number of transmit and receive coils can be used in order to balance the whole search head.

If we turn back to Figure 2.1, it was illustrated that a metallic object was placed beneath search head. This electrical conducting metal object will be subjected to magnetic field B_{tx} as well as received coil if it is placed near detector and a small current called eddy currents will be produced on it. Then, metallic object will create an opposing magnetic field, B_{target} due to flowing eddy currents on its surface. This situation is illustrated in the following figure.

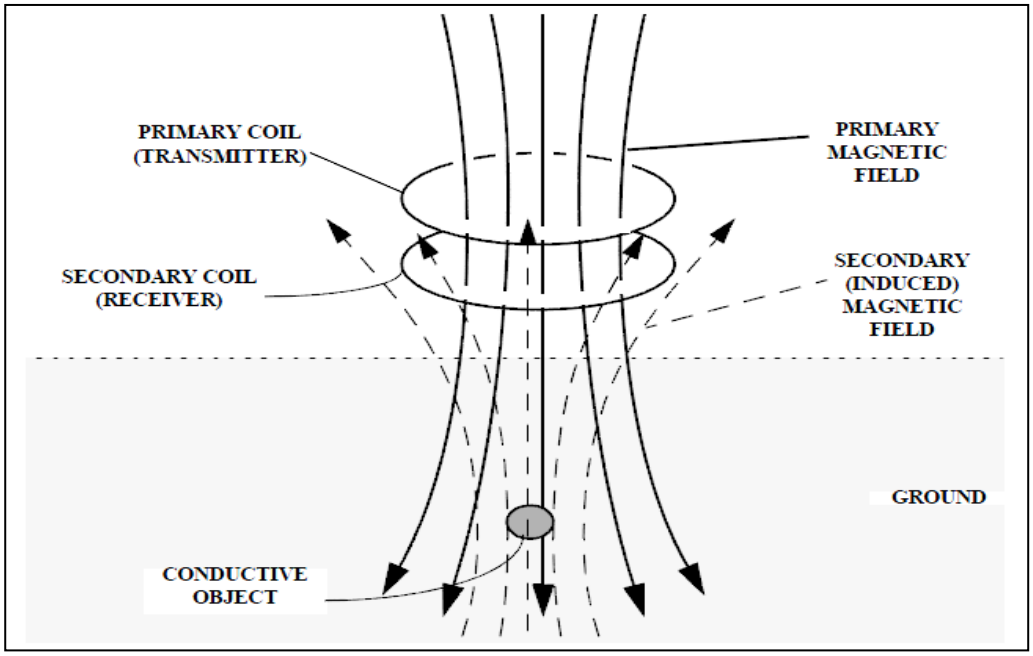

Figure 2.2. Illustration of magnetic fields on received coil due to transmit coil and metallic object beneath ground [2]

So, net magnetic field on the received coil(s) now can be expressed as sum of magnetic field produced by transmit coil(s); B_{tx}, and magnetic field produced by metallic target object; B_{target}

$$B_{rx} = B_{tx} + B_{target}$$

The secondary magnetic field due to target depends on a very large set of parameters, especially properties of object such as its shape, its dimension, its location and orientation underground, its electrical and magnetic characteristics (electrical conductivity, magnetic permeability). Properties of primary magnetic field caused by transmit coil(s) such as its temporal and spatial distribution, its magnitude over frequency are also important parameters that are related to secondary magnetic field. One of the most important parameters that can affect secondary magnetic field is electrical characteristics of ground wherein metallic object exists. Effects of different types of soils will be discussed more detailed in subsequent chapters.

2.2. PARAMETERS INFLUENCING THE INDUCED MAGNETIC FIELD

As it was mentioned before there are several parameters that affect secondary induced magnetic field and so induced current in the received coil.

Metal detectors are basically EM devices that are capable of detecting metallic buried objects in the ground. However, their detection capability is limited up to tens of centimeters to some meters depending of other determinative parameters. So, although direct contact of search head with ground is not necessary, a close proximity will be necessary considering limited depth detection. Also, generally metal detectors cannot give sufficient information about buried object (depth, shape, material etc.**)**.

Their inability for detecting objects which are buried deeper directly comes from the nature of magnetic field. As we know from Biot-Savart Law, magnetic field produced by a current carrying wire decreases very rapidly with the distance. As the strength of magnetic field is inversely proportional with square of distance, metal detectors will not be able to detect deeply buried objects unless produce a stronger magnetic field by transmitter coil. Also, in order to enhance detection depth, it requires larger accessory search coils or to give up attempts to eliminate trash metals. But, one must note that sensitivity of metal detector to desired objects will decrease as we use larger search heads. In other words, the larger the search coil, the deeper it can detect larger metal items but it is inconvenient to use in trashy areas with less depth to find small metal items.

Operating frequency of metal detectors is another important criterion for deeper detection. While lower frequency detectors offer better sensitivity to copper and silver and better overall detection, higher frequency detectors are not capable of detecting deeply buried objects although they are more sensitive to small metals and natural gold

How much an object has been absorbed into the soil is another factor in how deep the object can be detected. For example, iron objects tend to oxidize and become slowly absorbed into the surrounding material. This causes the target to appear larger and read-out more strongly, so it will be detected at greater depth with a metal detector, but this criterion is not important for gold targets because of less tendency of gold to oxidize.

Orientation of target has a great importance in the detection process. If we want to detect a coin, a coin lying flat (horizontal) can be detected more easily than an on-edge coil (vertical). It occurs just because horizontal coin offers more surface area and that means produce more eddy currents on its surface. So, it will be detected at a greater depth.

Electromagnetic properties of soil such as its magnetic permeability, dielectric permittivity, conductivity, thermal conductivity are the most important parameters that affect the operation of any type of metal detector. Also heat capacity, texture of soil and mineralization of soil are other parameters that can change detection performance. Effect of different types of soils for each coil type will be covered in detail in subsequent sections.

3. SIMULATION ANALYSIS

In this Chapter, simulation analysis will be covered specifically, how simulations are performed and what the design criteria are. Moreover, different types of coils will be examined in terms of their detection performance in the presence of certain metallic objects such as sphere, coin, nail etc. EM properties of different types of soils will be explained in detail.

All of the simulations in this part were realized in FEKO. FEKO was chosen for these simulations because of its Low Frequency Stabilization for Method of Moment (MoM). This feature gave us an opportunity to simulate our coil structures at very low frequencies with confidence. In order to test its capability, we did not use Low Frequency Stabilization in some structures and we realized that simulation results were incompatible with our theoretical expectations.

We have investigated and simulated ten distinct types of coils that are basically used in continuous wave metal detector's search heads. The illustration of these coil types and illustration of their FEKO models can be seen in the following figures. All structures have been simulated, but only for three of them we ran further simulations in order to understand their detection capabilities in different types of soil.

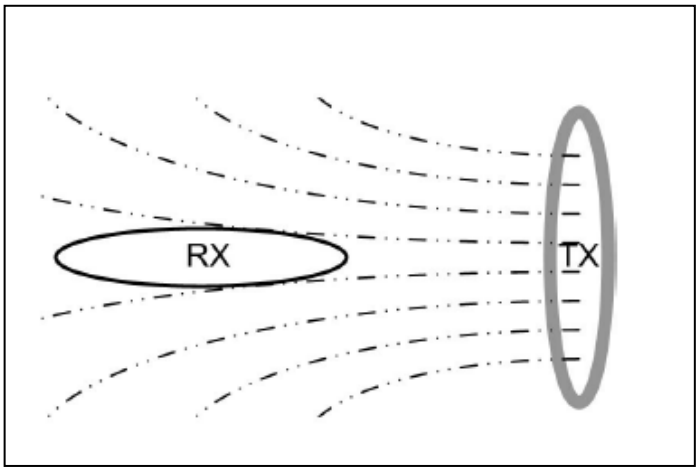

Figure 3.1. Orthogonal coils [12].

As mentioned in the previous section, the main challenge is to balance the receive coil so that the magnetic field of the transmit coil does not inductively couple to it. This balancing operation can be performed both designing coils properly and shielding the coils to avoid coupling. There are various ways to achieve mechanical balance and electrical balance in the receiver coil. For example orthogonal coil placement can be done for balancing receive coil as shown in Figure 3.1. It is one of the earliest methods of induction balance. Basically, transmit and receive coils are arranged orthogonally so that receive coil lies exactly along the isomagnetic lines of the transmit field. This way, the receive coil does not get any magnetic field cutting across it, and therefore very few induced current is expected. Inductive coupling is theoretically zero. The main disadvantage is that the orthogonal coil orientation results in a bulky search head.

In our simulations three different types of metallic objects were used as target. All of the targets were constructed from perfect electric conductor (PEC). Actually, we would like to construct those objects using different and more realistic materials such as copper, nickel coated material or iron etc. but the simulator did not allow us to use these properties while we use Low Frequency Stabilization feature.

First object that was created in FEKO is a sphere that has a radius of 10 mm and placed in the center axis of the coils in all of the simulations. Second one is a small cylindrical object created to represent a coin. It has a radius of 10 mm and a height of only 1 mm. We

selected third object, a nail as a more difficult target to detect to observe detection capabilities of coil designs properly. This nail is 25 mm in length and it was created by using a cone in the simulator. FEKO models of these metallic targets are illustrated in Figures 3.2, 3.3, and 3.4. Their dimensions are tabulated in Table 3.1

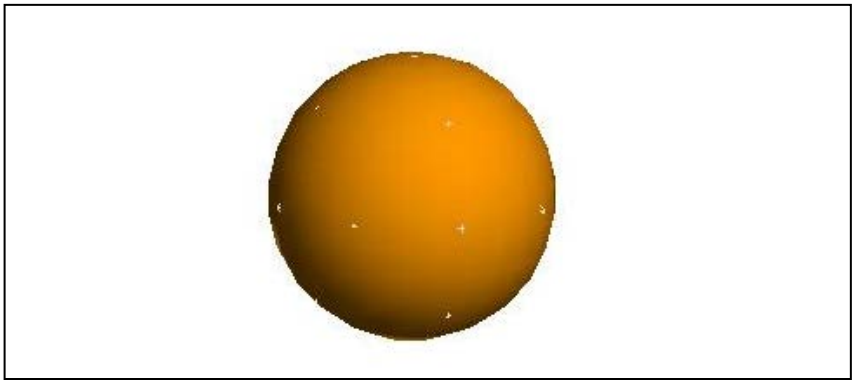

Figure 3.2. FEKO schematic of sphere target

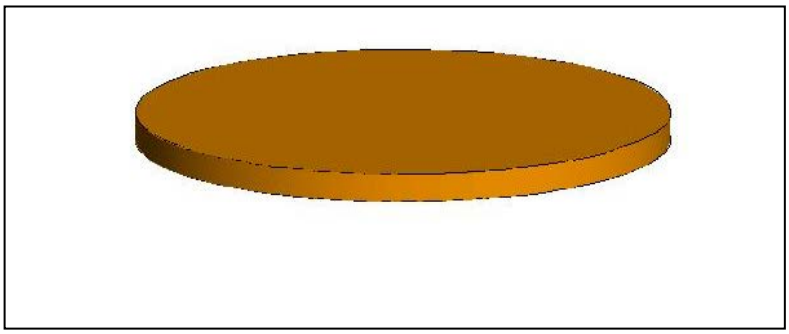

Figure 3.3. FEKO schematic of coin target

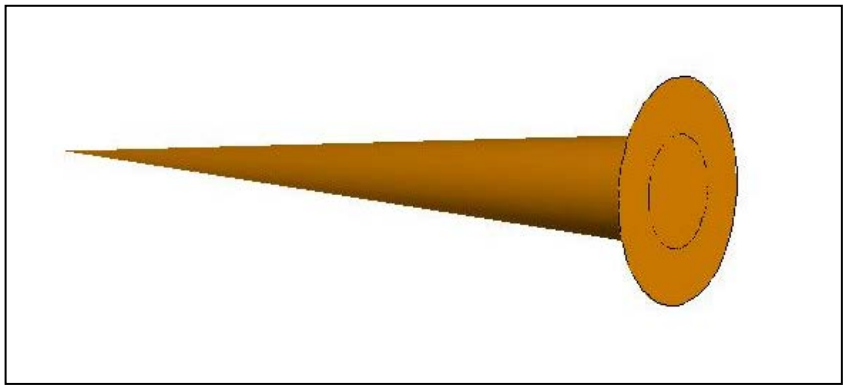

Figure 3.4. FEKO schematic of nail target

Table 3.1. Dimensions of metallic targets

	Sphere	Coin	Nail
Radius (mm)	10	10	-
Bottom Radius (mm)	-	-	0
Top Radius (mm)	-	-	3
Height (mm)	-	1	25

At first, we have simulated three selected coil structures in air with and without targets. Moreover, we have run some other simulations by creating different types of soils in FEKO to investigate detection characteristics of coils in various mediums. In order to simulate realistic deployment of metal detectors, we used dry soil, wet soil and ferrous soil in the simulations. Metallic objects have been placed under air-ground interface in FEKO at specific depths, and magnitude and phase of the receive port current were observed to get an idea how the response of coil changes with respect to electromagnetic characteristics of soil. All types of soils are represented in the model by using infinite plane feature of FEKO. This feature allowed us to form planar multilayer substrates with different medium types that are located at desired depths. An example illustration of soils can be seen in Figure 3.5.

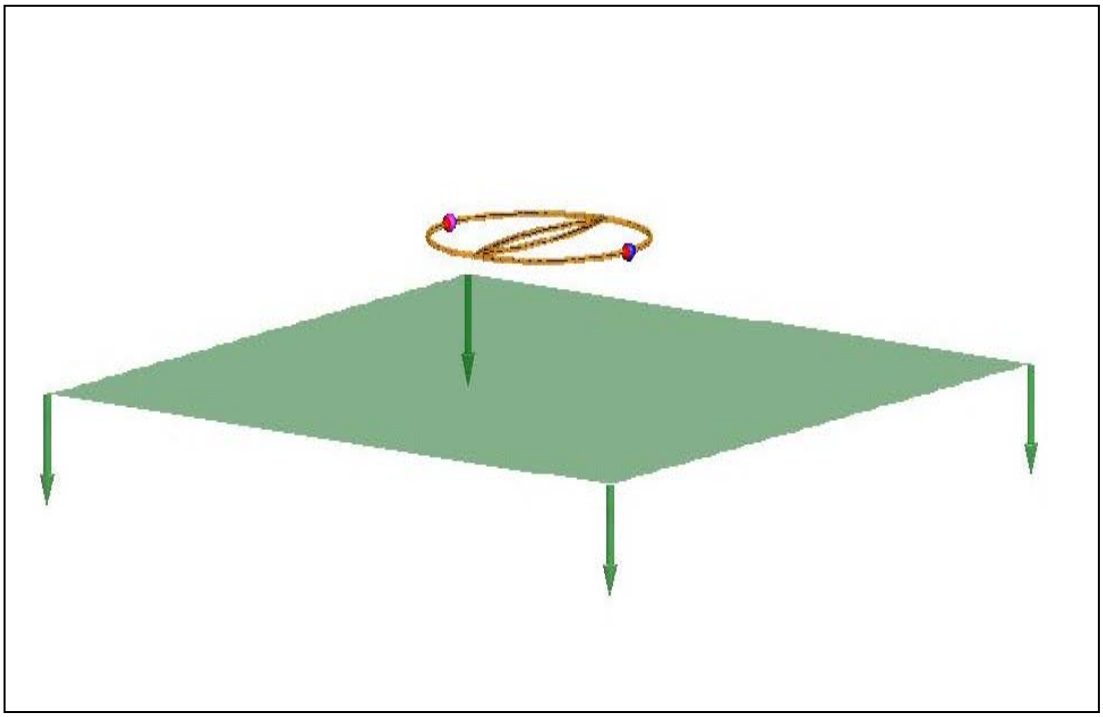

Figure 3.5. An example illustration of soil created by using infinite planes

Electrical properties of dry soil, wet soil and ferrous soil are tabulated in Table 3.2

Table 3.2. Electromagnetic properties of different types of soils

	Dry Soil	Wet Soil	Ferrous Soil
Relative Dielectric Permittivity	2.53	13	2.53
Conductivity (S/m)	0.01	0.06	0.01
Relative Magnetic Permeability	Non-magnetic	Non-magnetic	12
Mass Density (kg/m^3)	1000	1000	1000

3.1. OO TYPE COIL

First coil structure we have studied was the primitive OO-type coil structure as shown in Figure 3.6. To create this structure, receive coil (left one in the FEKO model) is overlapped a little bit with the transmit coil so that some amount of the inner field of the TX coil goes through the RX coil as well as some amount of the outer field of the TX coil which has opposite polarity with respect to inner field goes through the RX coil. Thus, a perfect arrangement of two coils will result in a balanced search head theoretically. In OO-type coil majority of EM field of transmit coil and receive coil is along their center axis. In other words they would have greatest sensitivity if they are to be deployed individually. Since axes of transmit and receive coils are not overlapped, greatest sensitivity will occur in the axes where two coils overlapped. But this results in a lower overall sensitivity and rare use of search heads which include OO-type coil.

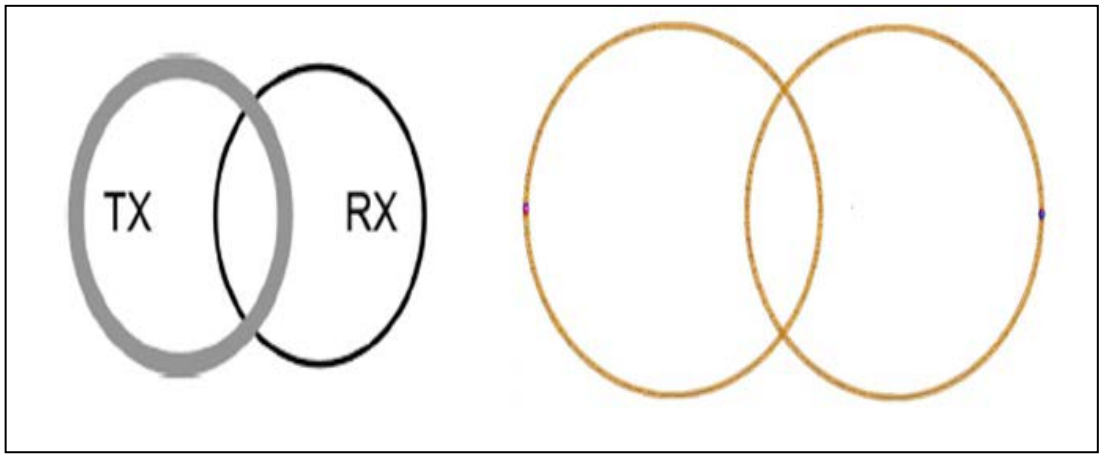

Figure 3.6. Illustration of OO-type coil (left), FEKO schematic of OO-type coil (right)

3.2. DD TYPE COIL

Another variation of the overlap design called DD-type is shown in Figure 3.7. This design has become very popular recently. The overlap areas of transmit and receive coils arranged and flattened in some way so that one can balance receive coil. Size of transmit coil nearly equals to size of receive coil as well as OO-type coil. Major advantages of this design are that it allows a longer detection zone and offers a deeper detection area especially in mineralized soil than OO-type coil. Also, they exhibit better performance in the separation of gold and other metals in ferrous soils.

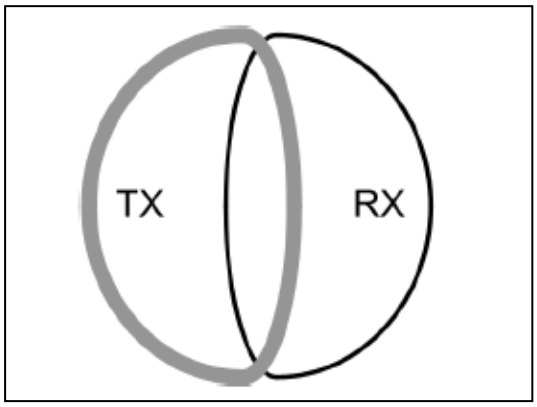

Figure 3.7. Illustration of DD-type coil

DD-type coil was one of our three coil designs that we simulated and studied in detail. FEKO model of our DD-type design is shown in Figure 3.8. Also, dimensions and properties of this design are tabulated in Table 3.3.

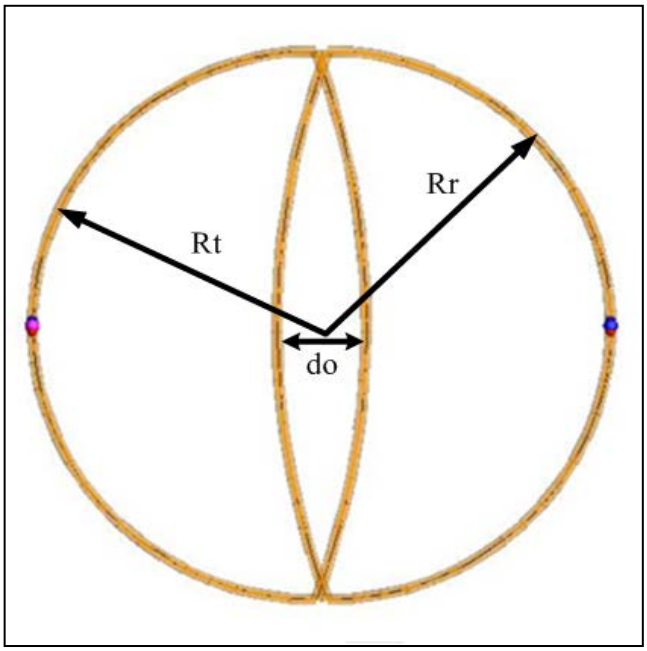

Figure 3.8. FEKO schematic of DD-type coil

Table 3.3. Dimensions of DD-type coil design

Radius of transmit coil (Rt)	100 mm
Radius of receive coil (Rr)	100 mm
Overlap of two-coils (do)	15.7 mm
Radius of wire	2 mm

Radii of coils were determined after an investigation of DD-type VLF continuous wave metal detectors. At first, overlap area of the structure arbitrarily decided. After a couple simulations and optimization processes realized by FEKO, 15.7 mm was found as optimum value for overlap parameter in order to achieve maximum balancing in receive coil. In the above figure left coil is transmit coil and is fed by 1V signal. Right one is receive coil and includes a port to measure induced current with or without metallic targets beneath soil.

After creating this type of coil, it was necessary to resonate coil at our operating frequency to maximize current in the receive port. As mentioned earlier at these frequencies we deploy our coils as inductors and we are not interested in their classical EM wave propagation properties. So, to make coils resonant, capacitor loads to the ports of transmit

and received coils have been added in parallel. Value of the necessary capacitors was calculated by using resonance formula of simple LC circuits at 150 kHz.

Firstly, we obtained the inductance value of coils in FEKO by running a simple simulation on air without the presence of any target, and then, we calculated necessary capacitance value to make the coil resonant.

Imaginary part of the simulated complex impedance of coil is nearly 353.7 mΩ. So, calculations to find capacitance become;

$$Z_L = j353.7\ \Omega$$

$$Z_L = j\ \omega\ L$$

$$j353.7 = j\ \omega\ L$$

$$\omega = 2\ \pi\ f$$

$$f = 150\ kHz$$

$$j353.7 = j2\pi(150\ x\ 10^3)L$$

So, L becomes,

$$L = 0.37\ x\ 10^{-6}\ H$$

From the resonance formula,

$$f = \frac{1}{2\ \pi\ \sqrt{L\ C}}$$

$$150\ x\ 10^3 = \frac{1}{2\ \pi\ \sqrt{0.37\ x\ 10^{-6}.\ C}}$$

So, necessary capacitance value becomes,

$$C = 3.04\ x\ 10^{-6}\ F$$

Thus, all simulations have been performed after a capacitor has a value of $3.04\ x\ 10^{-6}\ F$ and a 1 Ω resistor were placed as a parallel load to the ports of DD type coils.

3.3. COAXIAL TYPE COIL

Coaxial type coil structure is illustrated in Figure 3.9. This type has one of the most successful arrangement of transmit and receive coils to achieve balance in receive coil. It is called as coaxial coil since all of coils lie along the nearly same axis. Basically, two different types of coaxial coil exist. One of them consists of a transmit coil between two received coils (Figure 3.9 left) and the other configuration consists of a transmit coil between two receive coils. (Figure 3.9 right). Although both of them constructed and simulated in FEKO, it will be given the results of the configuration that includes two receive coils and one transmit coil.

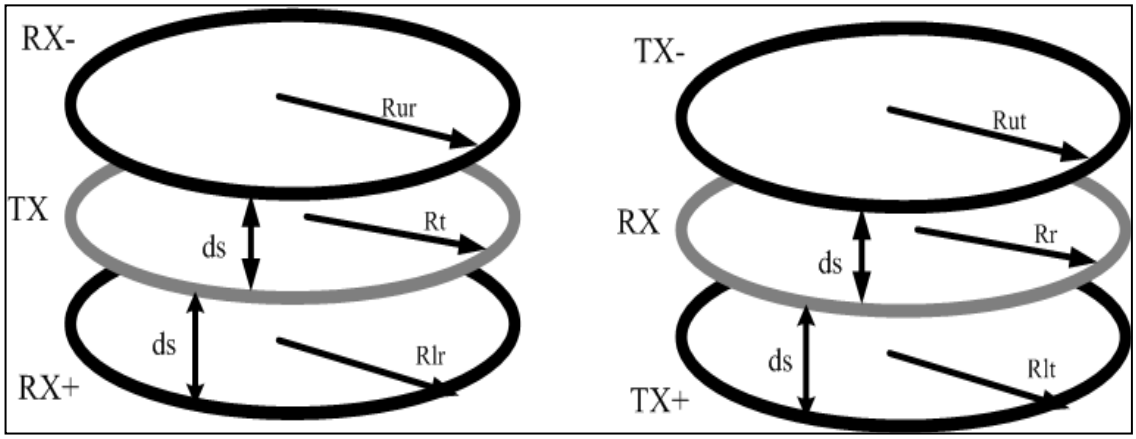

Figure 3. 9. Illustration of two different types of coaxial coil

In this configuration the transmit coil is placed between two receive coils at a specific point so that total induced current of received coil 1 and received coil 2 produced by transmit coil will cancel each other. Alternatively, if one constructs two transmit coils in opposite then the induced current on the received coil that is sandwiched by two opposing transmit coils will be nearly zero. In both configurations main idea is placing three coils such that their fields cancel out on the receive coil(s). Generally, size of transmit and receive coils are same to achieve maximum balance. However, there are some other designs which use smaller receive coils than transmit coils. It causes a worse induction balance performance but improves detection performance of small objects in close proximity by reducing magnitude of the unwanted ground signal.

Main advantage of coaxial coil arrangement is its nearly perfect induction balance. Thanks to its induction balance that occurs in vertical direction, it offers better separation of non-worthy materials and desirable targets in close proximity. Also, induction balance in vertical axis provides a greater capability of search near metallic fences without causing a false alarm. However, it has a certain drawback that it can only provide a small detection depth since a significant amount of signal cancellation occurs between two "+" polarized coil and "-" polarized coil.

Coaxial type coil with two receive coils and a transmit coil was another selected design that we simulated and studied in details. In Figure 3.10, FEKO model of our coaxial type design can be seen. Also, dimensions and properties of this design are tabulated in Table 3.4.

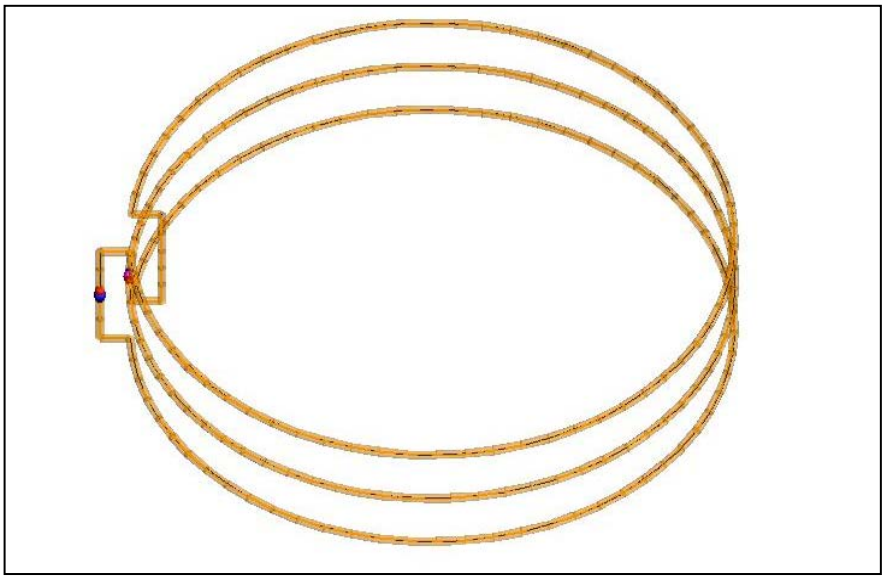

Figure 3.10. FEKO schematic of coaxial type coil

Table 3. 4 Dimensions of coaxial type coil design

Radius of transmit coil (Rt)	100 mm
Radius of upper receive coil (Rur)	100 mm
Radius of lower receive coil (Rlr)	100 mm
Spacing between coils (ds)	20 mm
Radius of wires	1.5 mm

Radii of coils were selected same as radii of DD-type coils to be able to make proper comparison between the two types. At first, spacing between coils was arbitrarily decided but after a couple simulations and optimization, it was concluded as 20 mm to achieve induction balance as much as possible. In the above model coil placed in the middle is transmit coil and is fed by 1V signal. The other coils are receive coils and connected to each other via a port to measure induced current during simulations.

Again, it was necessary to resonate coil at our operating frequency to maximize current in the receive port in the presence of a metallic target. We performed the same operations as in DD-type coil to find necessary capacitance value to make the coil resonant at 150 kHz.

Imaginary part of the simulated complex impedance of coil was nearly 353.7 mΩ. The capacitance becomes;

$$Z_L = j509\ \Omega$$

$$Z_L = j\ \omega\ L$$

$$j509 = j\ \omega\ L$$

$$\omega = 2\ \pi\ f$$

$$f = 150\ kHz$$

$$j509 = j2\pi(150\ x\ 10^3)L$$

Hence, L is,

$$L = 0.54\ x\ 10^{-6}\ H$$

From the resonance formula,

$$f = \frac{1}{2\ \pi\ \sqrt{L\ C}}$$

$$150\ x\ 10^3 = \frac{1}{2\ \pi\ \sqrt{0.54\ x\ 10^{-6}.\ C}}$$

So, the necessary capacitance value becomes,

$$C = 2.11\ x\ 10^{-6}\ F$$

Thus, all simulations have been performed after a capacitor value of $2.11\ x\ 10^{-6}\ F$, and a 1 Ω resistor were placed as a parallel load to the ports of coaxial type coils.

3.4. 8-SHAPED TYPE COIL

8-shaped coil structures for different configurations are shown in Figure 3.11. The leftmost configuration has the transmit coil twisted just like number “8” so that it will produce opposing magnetic fields on the receive coil and it is expected that the receive coil has induction balance since it is centered at the crossover of transmit coil.

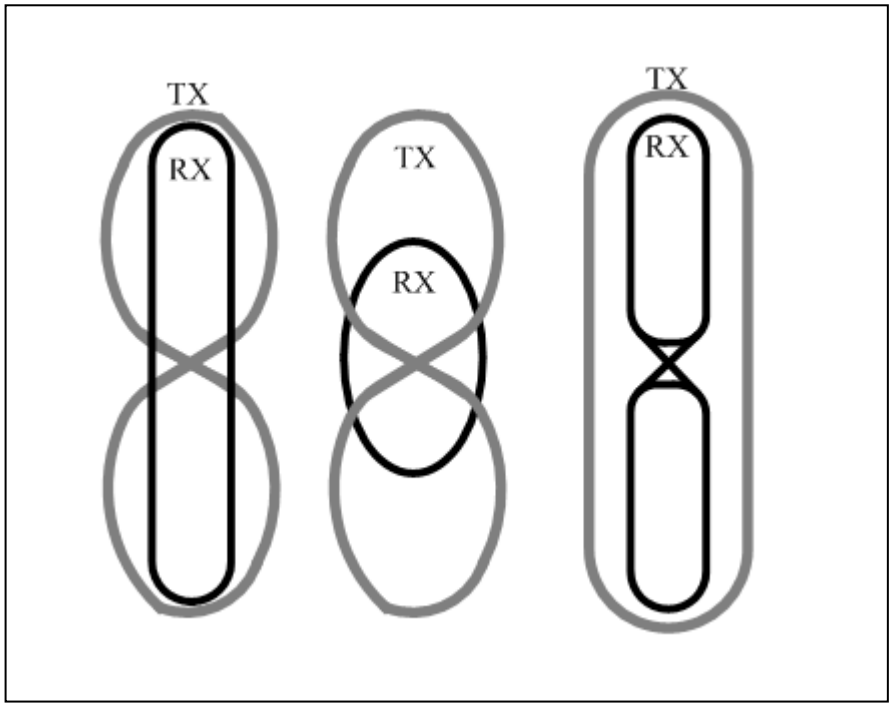

Figure 3.11. Illustration of three different types of 8-shaped coil

Advantage of this configuration is that a good induction balance can be obtained if transmit and receive coils are placed properly. On the other hand this coil configuration has an important disadvantage that magnetic field created by transmit coil has a null at the crossover. It is a disadvantage because it will cause very poor detection sensitivity at the main axes of the search head. Another disadvantage of 8-shaped coils is they have a dependency to exact placement of transmit and receive coils in order to sustain induction balance. That means little movements of coils will affect the detection performance of 8-shaped coils dramatically.

Another configuration can be seen in Figure 3.11 in the middle. It has the same transmit coil with first configuration but the difference comes from that has an elongated receive

coil instead of an elliptical one. This configuration has similar disadvantages with first configuration but it can offer a long and narrow search area because of having an elongated receive coil.

Third configuration in Figure 3.11 (right) was selected for simulations. It has an 8-shaped receive soil, alternatively but its main characteristics are very similar to other configurations of 8-shaped coils. But, since we already knew that this configuration would show a very bad detection performance for the targets placed along the center axis because of its drawback, metallic targets were not placed in the center of the overall coil instead placed in the center of upper part of the transmit and elongated receive coil for only 8-shaped type coil. FEKO model of coil geometry and a spherical target placed in the previously mentioned place can be seen in Figure 3.12.

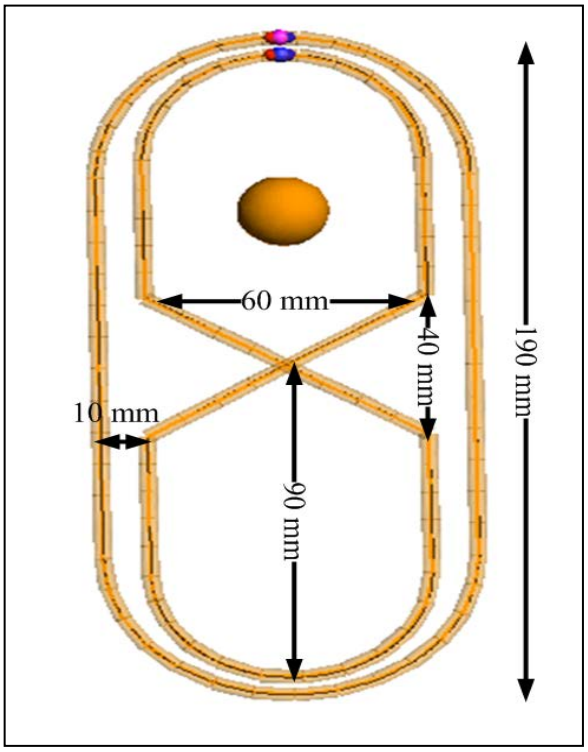

Figure 3.12. FEKO model of 8-shaped type coil with a spherical target placed in the center axis of the upper part of the transmit and elongated receive coil

In the above configuration, outer elongated coil is transmit-coil and inner 8-shaped coil is receive-coil. The total length of the transmit coil is 190mm and total length of receive coil is about 180 mm. Width of the transmit coil was selected as 80 mm at the widest point and width of received coil was selected as 60 mm. These values were selected both to be able to make proper comparisons with other types of coils and to achieve maximum possible induction balance on the receive coil. Outer transmit is fed by 1V signal. To 8-shaped receive coil, a port is connected to measure induced current during simulations.

Again, it was necessary to resonate coil at our operating frequency to maximize current in the receive port in the presence of a metallic target. We performed the same operations as in other types of coils to find necessary capacitance value to make the coil resonant at 150 kHz.

Imaginary part of the simulated complex impedance of coil is nearly 415.8 mΩ. The capacitance becomes;

$$Z_L = j416\ \Omega$$

$$Z_L = j\ \omega\ L$$

$$j415 = j\ \omega\ L$$

$$\omega = 2\ \pi\ f$$

$$f\ = 150\ kHz$$

$$j415 = j2\pi(150\ x\ 10^3)L$$

So, L becomes,

$$L = 0.44\ x\ 10^{-6}\ H$$

From the resonance formula,

$$f = \frac{1}{2\,\pi\,\sqrt{L\,C}}$$

$$150\ x\ 10^{3} = \frac{1}{2\,\pi\,\sqrt{0.44\ x\ 10^{-6}.\,C}}$$

So, necessary capacitance value becomes,

$$C = 2.55\ x\ 10^{-6}\ F$$

Thus, all simulations have been performed after a capacitor value of $2.55\ x\ 10^{-6}\ F$ and a 1 Ω resistor were placed as a parallel load to the ports of 8-shaped type coil.

3.5. 4B TYPE COIL

4B type coil was another configuration it has been studied and modeled in FEKO. FEKO model of 4B type is illustrated in Figure 3.13. This coplanar coil design was widely used. It does not have a frequent usage in modern VLF metal detectors. It is created by folding transmit coil a little bit inward and placing receive coil across the folding axis of transmit coil. In this configuration it is expected that the folded part of the transmit coil will create an opposing magnetic field to non-folded part of transmit coil. So, these two reverse fields will cancel each other on the receive coil.

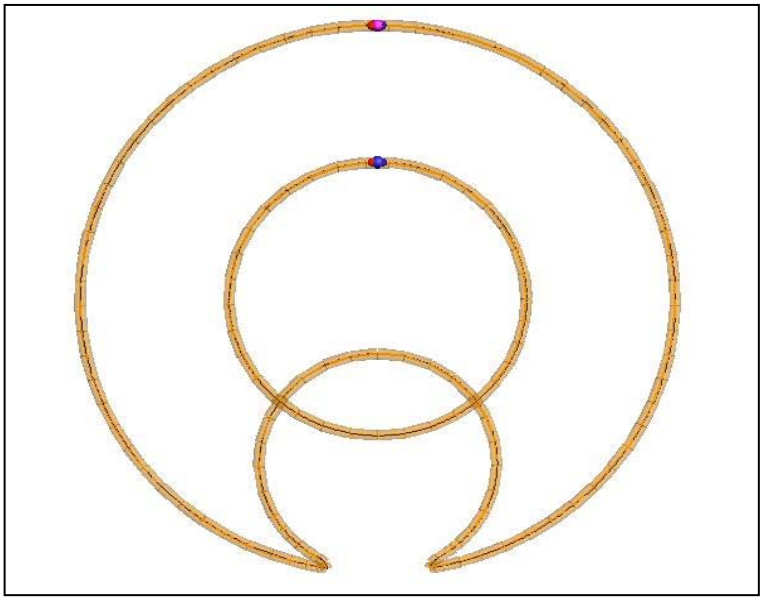

Figure 3.13. FEKO model of 4B-type coil

3.6. CONCENTRIC COILS

Concentric coils are widely used in today's metal detectors. The concentric configuration consists of transmit coil(s) and receive coil(s) that are arranged as shown in Figure 3.14. Main goal to place and configure the coils as shown in the figure is exactly the same with other types; achieving maximum induction balance. Principal advantage of this configuration is that it offers a significant detection depth and also offers the most symmetrical detection area since transmit and receive coils are perfectly circular. On the other hand, concentric coils are the most sensitive type of coils to unwanted ground signals and this gives a very poor detection capability in mineralized soils.

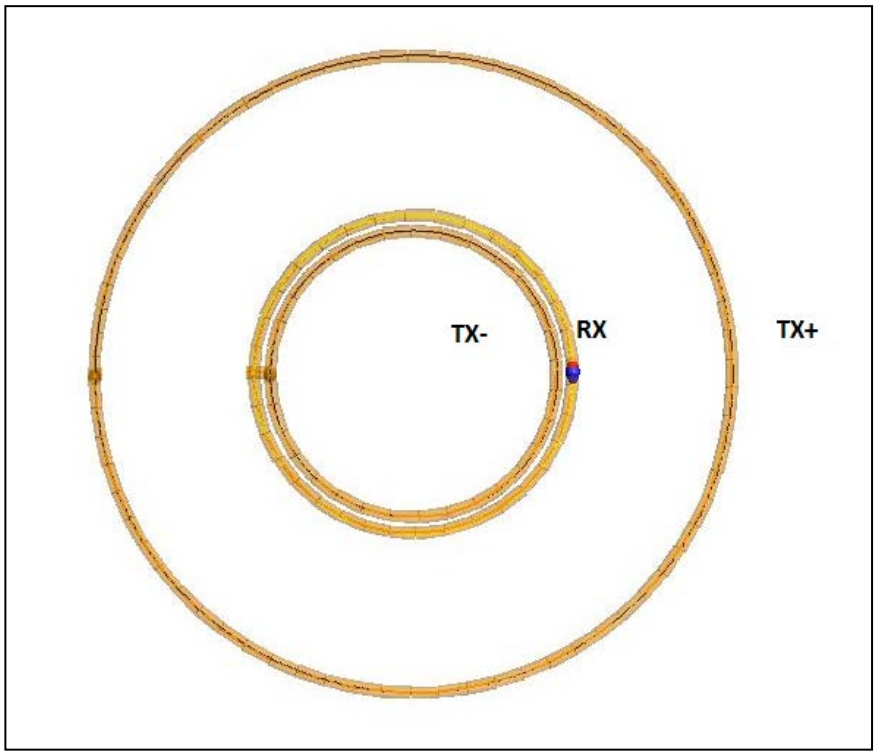

Figure 3.14. FEKO model of concentric type coil

4. RESULTS AND DISCUSSION

Three type of coils; DD-type coil, coaxial type coil and 8-shaped type coil have been simulated and their results are tabulated in the following tables.

At first, simulations were performed on air to get an initial idea about how much they are balanced. These simulations also give us an idea for detection capabilities of different types of coils at certain depths. As metallic targets, three distinct objects were defined as explained in Section 3.

4.1. ON AIR SIMULATIONS

4.1.1. DD-type coil

In Table 4.1 simulation results are tabulated for DD-type coil. d_t represents the vertical distance between center of coil and the location of metallic target and Δ represents the difference between the magnitude of current with target at related depth and magnitude of current without target. Also, Δ represents the difference between phase of current with target at related depth and phase of current without target to at what rate they have been changed.

Table 4.1. Receive port induced current of DD-type coil on air

	Sphere(PEC)		Coin(PEC)		Nail(PEC)	
	Magnitude	Phase(deg)	Magnitude	Phase(deg)	Magnitude	Phase(deg)
Without target	20.2236 mA	54.8077	20.2236 mA	54.8077	20.2236 mA	54.8077
d_t =80mm	19.6552 mA Δ=0.5684 mA	54.8233 Δ=- 0.0156	19.7009 mA Δ=0.5227 mA	54.8152 Δ=- 0.0075	20.1702 mA Δ=0.0534 mA	54.8092 Δ=- 0.0015
d_t =130mm	20.0812 mA Δ=0.1424 mA	54.8103 Δ=-0.0026	20.1196 mA Δ=0.104 mA	54.8092 Δ=- 0.0015	20.2105 mA Δ=0.0131 mA	54.808 Δ=- 0.0003
d_t =150mm	20.1413 mA Δ=0.0823 mA	54.8091 Δ=-0.0014	20.1658 mA Δ=0.0578 mA	54.8085 Δ=- 0.0008	20.216 mA Δ=0.0076 mA	54.8079 Δ=- 0.0002
d_t =180mm	20.1859 mA	54.8083	20.198 mA	54.8081	20.2201 mA	54.8078

	Δ=0.0377 mA	Δ=-0.0006	Δ=0.0256 mA	Δ=- 0.0004	Δ=0.0035 mA	Δ=- 0.0001
d_t =200mm	20.2004 mA Δ=0.0232 mA	54.8081 Δ=-0.0004	20.2081 mA Δ=0.0155 mA	54.808 Δ=- 0.0003	20.2214 mA Δ=0.0022 mA	54.8078 Δ=- 0.0001
d_t =230mm	20.2118 mA Δ=0.0118 mA	54.8079 Δ=-0.0002	20.2159 mA Δ=0.0077 mA	54.8079 Δ=- 0.0002	20.2225 mA Δ=0.0011 mA	54.8078 Δ=- 0.0001
d_t =250mm	20.2159 mA Δ=0.0077 mA	54.8079 Δ=-0.0002	20.2186 mA Δ=0.005 mA	54.8078 Δ=- 0.0001	20.2229 mA Δ=0.0007 mA	54.8078 Δ=- 0.0001
d_t =300mm	20.2206 mA Δ=0.003 mA	54.8078 Δ=-0.0001	20.2217 mA Δ=0.0019 mA	54.8078 Δ=- 0.0001	20.2233 mA Δ=0.0003 mA	54.8078 Δ=- 0.0001
d_t =350mm	20.2223 mA Δ=0.0013 mA	54.8078 Δ=-0.0001	20.2227 mA Δ=0.0009 mA	54.8078 Δ=- 0.0001	20.2234 mA Δ=0.0002 mA	54.8078 Δ=- 0.0001
d_t =400mm	20.223 mA Δ=0.0006 mA	54.8078 Δ=-0.0001	20.2232 mA Δ=0.0004 mA	54.8078 Δ=- 0.0001	20.2235 mA Δ=0.0001 mA	54.8078 Δ=- 0.0001
d_t=450mm	20.2232 mA Δ=0.0004 mA	54.8078 Δ=-0.0001	20.2234 mA Δ=0.0002 mA	54.8078 Δ=- 0.0001	20.2235 mA Δ=0.0001 mA	54.8077 Δ=0
d_t =500mm	20.2234 mA Δ=0.0002 mA	54.8078 Δ=-0.0001	20.2235 mA Δ=0.0001 mA	54.8078 Δ=- 0.0001	20.2235 mA Δ=0.0001 mA	54.8077 Δ=0

As it can be seen from above table, DD-type coil does not have a satisfactory induction balance as expected. We can observe this by looking the value of receive port current in the receive coil when there is no target that is 20.2236 mA. However, it gives a longer detection since it runs from back to front of coil and offers a deeper detection area. It can detect a PEC defined sphere with 10 mm radius at a vertical distance 500 mm from the center of the coil although it has only one turn. We can understand this by looking the difference between current magnitudes when there is no target and d_t =500 mm. There is a very small difference between two current values in the order of μA. But in a more realistic design, if we use transmit and receive coils with 23 turns than we would obtain a current difference in the order of mA since receive currents in both circumstances are directly proportional to square of turns ratio as it is already discussed in Section 2. In this way this current would be big enough to create an alarm after amplified.

This coil can easily detect objects up to d_t= 200 mm according to simulation results. After that distance, difference between currents when there is no target and with a target at that distance is getting smaller and smaller. It is obvious that after d_t=500 mm our coil cannot detect any of these targets since the magnitude of current becomes equal to without target condition.

Another point to note in these results is that the coil can detect sphere target more easily than other targets since sphere has the biggest surface area. It is an expected result regarding to Section 2.1 that reverse magnetic field created by target occurs under influence of eddy currents and eddy currents flow on the surface of object. So, the bigger surface of object, more eddy current flows on surface and create more reverse magnetic field on receive coil. According to results nail is the most difficult target object to detect by far since it has a very small surface area compared to others. Phase of receive port current has nearly no variation with respect to d_t on air simulations.

4.1.2. Coaxial type coil

In Table 4.2 simulation results are tabulated for coaxial type coil where d_t represents the vertical distance between center of coil and the location of metallic target.

Table 4. 2. Receive port induced current of coaxial type coil on air

	Sphere(PEC)		Coin(PEC)		Nail(PEC)	
	Magnitude	Phase(deg)	Magnitude	Phase(deg)	Magnitude	Phase(deg)
Without target	12.2357 nA	-9.45875	12.2357 nA	-9.45875	12.2357 nA	-9.45875
d_t =80mm	171.785 µA	169.629	101.114 µA	169.626	16.1056 µA	169.622
d_t =130mm	39.4844 µA	169.623	24.5492 µA	169.623	3.61838 µA	169.619
d_t =150mm	21.4028 µA	169.622	13.3101 µA	169.622	1.95888 µA	169.616
d_t =180mm	8.85568 µA	169.621	5.50273 µA	169.62	811.957 nA	169.608
d_t =200mm	5.08159 µA	169.62	3.15189 µA	169.619	466.179 nA	169.597
d_t =230mm	2.32489 µA	169.617	1.44288 µA	169.614	215.14 nA	169.568
d_t =250mm	1.43078 µA	169.614	888.105 nA	169.609	136.744 nA	169.537
d_t =300mm	474.38 nA	169.598	293.003 nA	169.582	41.5449 nA	169.341
d_t =350mm	179.214 nA	169.557	104.154 nA	169.51	14.847 nA	168.837
d_t =400mm	76.46 nA	169.47	42.217 nA	169.346	8.35737 nA	168.227
d_t =450mm	30.687 nA	169.242	23.7686 nA	169.132	2.84813 nA	165.526
d_t =500mm	18.8736 nA	169.004	13.222 nA	168.74	5.42098 nA	167.471

As it can be seen from above table coaxial type coil has a much better induction balance performance compared to DD-type coil. It can be observed by looking the magnitude of

receive port current when there is no target. It has a value in the order of nA and this relatively small value guarantees a nearly perfect induction balance as expected. Then, a metallic target will produce a bigger difference in current and so detection capability of coil will be improved. Simulation results with target at a proximity coil shows us receive port current changes in the order of 1000 with the presence of a target. Again having a multi-turn coil will increase this current significantly and an alarm will be occurred in metal detector.

Similar to DD-type coil its detection capability diminishes with increasing depth but decrement in the receive port difference occurs in a very fast way. Magnitude of current decreases dramatically as d_t gets bigger. This was an expected result discussed in Section 3.3 that coaxial type coil offers a better performance for objects in a close proximity but has a drawback to detect deeply buried objects since significant amount of signal cancellation occurs between two “+” polarized coil and “-” polarized coil.

Detection capability depending on form and surface area of object in DD-type is also valid in coaxial type coil. It can be seen easily by looking to simulation results on above table.

Phase of receive port current has nearly no variation with respect to d_t on air simulations but it must be noted that there is almost 180° phase difference between with target and without target conditions.

4.1.3. 8-shaped type coil

In Table 4.3 simulation results are tabulated for 8-shaped type coil where d_t represents the vertical distance between center of coil and the location of metallic target.

Table 4. 3. Receive port induced current of 8-shaped type coil on air

	Sphere(PEC)		Coin(PEC)		Nail(PEC)	
	Magnitude	Phase(deg)	Magnitude	Phase(deg)	Magnitude	Phase(deg)
Without target	16.3334 mA	-12.0212	16.3334 mA	-12.0212	16.3334 mA	-12.0212
d_t =80mm	16.2745 mA	-11.8945	16.2971 mA	-11.9433	16.3279 mA	-12.0094
d_t =130mm	16.3311 mA	-12.0152	16.3244 mA	-12.0004	16.3321 mA	-12.018
d_t =150mm	16.3331 mA	-12.0206	16.332 mA	-12.0176	16.3330 mA	-12.0207
d_t =180mm	16.3332 mA	-12.0209	16.3333 mA	-12.0208	16.3333 mA	-12.0212
d_t =200mm	16.3333 mA	-12.0211	16.3334 mA	-12.0212	16.3334 mA	-12.0212
d_t =230mm	16.3334 mA	-12.0212	16.3334 mA	-12.0212	16.3334 mA	-12.0212
d_t =250mm	16.3334 mA	-12.0212	16.3334 mA	-12.0212	16.3334 mA	-12.0212
d_t =300mm	16.3334 mA	-12.0212	16.3334 mA	-12.0212	16.3334 mA	-12.0212
d_t =350mm	16.3334 mA	-12.0212	16.3334 mA	-12.0212	16.3334 mA	-12.0212
d_t =400mm	16.3334 mA	-12.0212	16.3334 mA	-12.0212	16.3334 mA	-12.0212
d_t =450mm	16.3334 mA	-12.0212	16.3334 mA	-12.0212	16.3334 mA	-12.0212
d_t =500mm	16.3334 mA	-12.0212	16.3334 mA	-12.0212	16.3334 mA	-12.0212

As it can be seen from above table 8-shaped type coil has the worst induction balance performance among three configurations. It can be observed by looking the magnitude of receive port current when there is no target. It has a value in the order of mA. This situation is the result of great dependency of induction balance to exact placement of coils in this type. Also one can see easily from above table that it has not a sufficient detection performance even if the target is placed in a close proximity of coil. We saw these results although metallic targets were not placed in the center of the overall coil instead placed along the center of upper part of the transmit and elongated receive coil for only 8-shaped type coil to overcome the null of magnetic field produced by transmit coil in the center of upper and lower transmit coils. Actually, a couple of simulations were performed by placing targets at the crossover to see how do differ results and its detection capability is worse than as expected compared to placing targets in the center of upper transmit coil only. For example, 8-shaped coil could not detect targets after d_t exceeds 100 mm for all types of targets when they were placed at the crossover but after moving them to the current place, it has been seen that there is a little upturn in detection range and it now can detect targets up to 200 mm.

4.2. DRY SOIL SIMULATIONS

Second step in our simulation process was simulating all structures in more realistic environments. First case was locating objects under dry soil at specific depths. Background and analysis of this simulation has already been made in Section 3. In the following tables simulation results can be seen where d_t represents the distance from surface of ground layer to metallic target and d_c represents the distance from center of coil to surface of ground. Simulation results at for different d_c and d_t values are tabulated in the following four tables.

4.2.1. DD-type coil

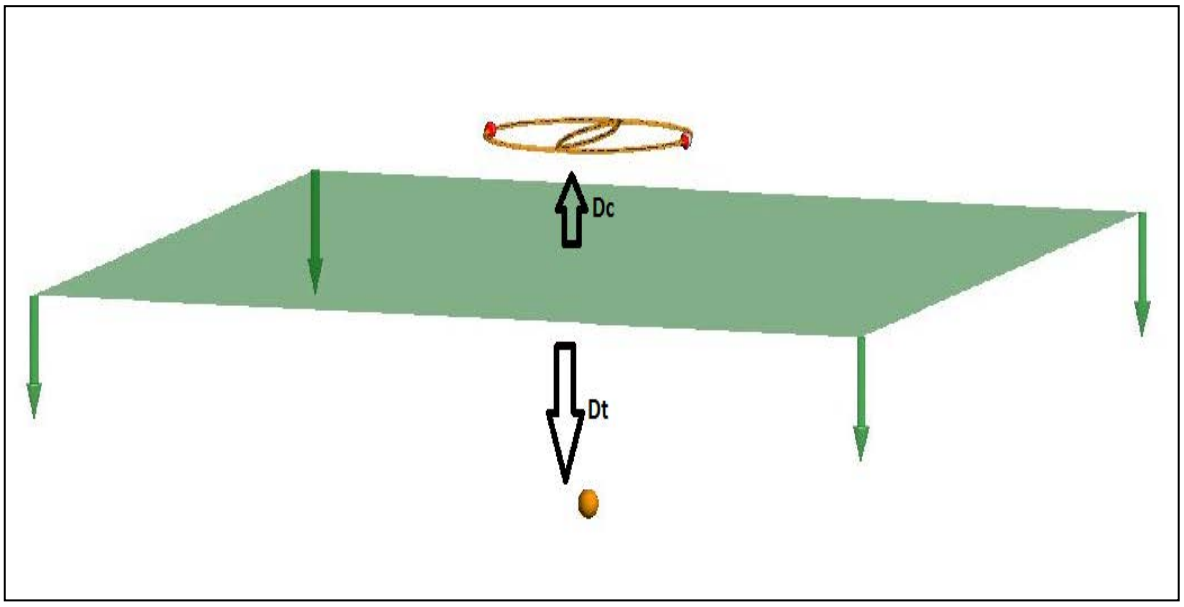

Figure 4. 1. FEKO model of simulation setup with DD-type coil in dry soil

Table 4. 4. Receive port induced current of DD-type coil at d_c = 50 mm in dry soil

d_c= 50 mm	Sphere(PEC)		Coin(PEC)		Nail(PEC)	
	Magnitude	Phase(deg)	Magnitude	Phase(deg)	Magnitude	Phase(deg)
Without target	12.3046 mA	53.6182	12.3046 mA	53.6182	12.3046 mA	53.6182
d_t =30mm	11.7389 mA	53.6276	11.7845 mA	53.6199	12.2515 mA	53.6191
d_t =100mm	12.2228 mA	53.6188	12.2471 mA	53.6184	12.2971 mA	53.6183
d_t =300mm	12.3033 mA	53.6182	12.3038 mA	53.6182	12.3045 mA	53.6182

Table 4. 5. Receive port induced current of DD-type coil at d_c = 100 mm in dry soil

d_c=100mm	Sphere(PEC)		Coin(PEC)		Nail(PEC)	
	Magnitude	Phase(deg)	Magnitude	Phase(deg)	Magnitude	Phase(deg)
Without target	12.3047 mA	53.6593	12.3047 mA	53.6593	12.3047 mA	53.6593
d_t =30mm	12.1631 mA	53.6608	12.2013 mA	53.6599	12.2917 mA	53.6594
d_t =100mm	12.2816 mA	53.6595	12.2893 mA	53.6594	12.3026 mA	53.6593
d_t =300mm	12.3041 mA	53.6593	12.3043 mA	53.6593	12.3046 mA	53.6593

Table 4. 6. Receive port induced current of DD-type coil at d_c = 150 mm in dry soil

d_c=150mm	Sphere(PEC)		Coin(PEC)		Nail(PEC)	
	Magnitude	Phase(deg)	Magnitude	Phase(deg)	Magnitude	Phase(deg)
Without target	12.3047	53.6802	12.3047 mA	53.6802	12.3047	53.6802
d_t =30mm	12.2672 mA	53.6806	12.2793 mA	53.6804	12.3013 mA	53.6802
d_t =100mm	12.2971 mA	53.6802	12.2998 mA	53.6802	12.304 mA	53.6802
d_t =300mm	12.3044 mA	53.6802	12.3045 mA	53.6802	12.3047 mA	53.6802

Table 4. 7. Receive port induced current of DD-type coil at d_c = 200 mm in dry soil

d_c=200mm	Sphere(PEC)		Coin(PEC)		Nail(PEC)	
	Magnitude	Phase(deg)	Magnitude	Phase(deg)	Magnitude	Phase(deg)
Without target	12.305 mA	53.7048	12.305 mA	53.7048	12.305 mA	53.7048
d_t =30mm	12.2933 mA	53.705	12.2973 mA	53.7049	12.3039 mA	53.7048
d_t=100mm	12.302 mA	53.7049	12.3031 mA	53.7049	12.3047 mA	53.7048
d_t=300mm	12.3048 mA	53.7048	12.3049 mA	53.7048	12.305 mA	53.7048

4.2.2. Coaxial type coil

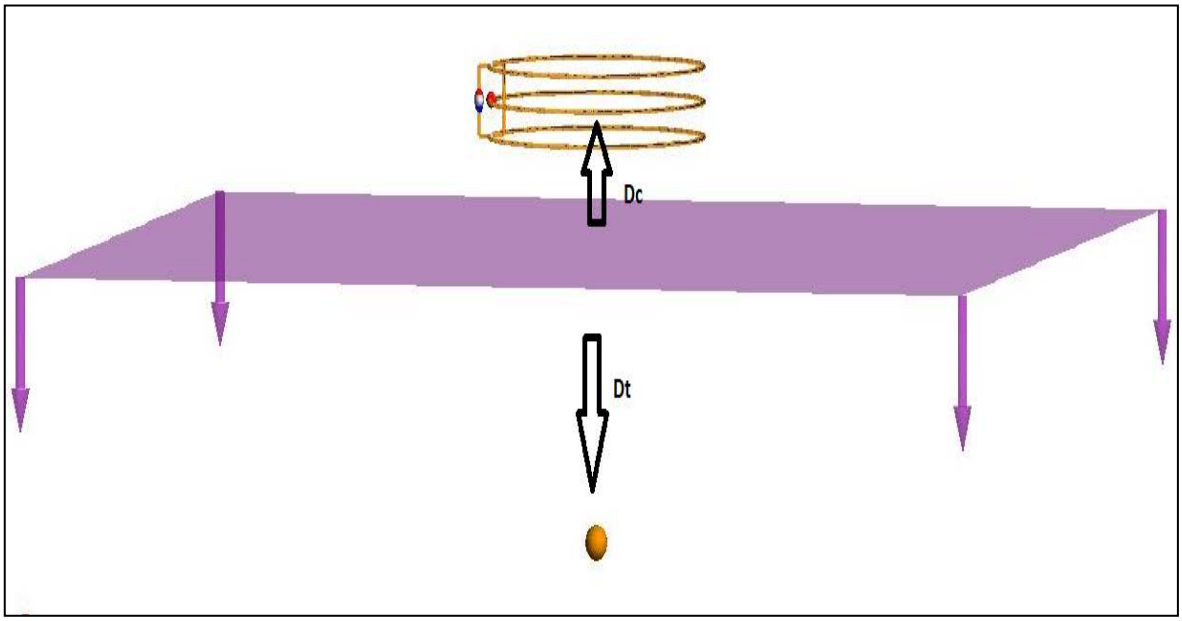

Figure 4. 2. FEKO model of simulation setup with coaxial type coil

Table 4. 8. Receive port induced current of coaxial type coil at d_c = 50 mm in dry soil

d_c=50mm	Sphere(PEC)		Coin(PEC)		Nail(PEC)	
	Magnitude	Phase(deg)	Magnitude	Phase(deg)	Magnitude	Phase(deg)
Without target	1.3223 μA	-128.313	1.3223 μA	-128.313	1.3223 μA	-128.313
d_t =30mm	171.492 μA	169.685	107.166 μA	169.918	16.6766 μA	173.317
d_t=100mm	21.9299 μA	172.346	13.8966 μA	174.12	2.82254 μA	-166.187
d_t=300mm	1.4112 μA	-134.585	1.37507 μA	-132.268	1.33057 μA	-128.987

Table 4. 9. Receive port induced current of coaxial type coil at d_c = 100 mm in dry soil

d_c=100mm	Sphere(PEC)		Coin(PEC)		Nail(PEC)	
	Magnitude	Phase(deg)	Magnitude	Phase(deg)	Magnitude	Phase(deg)
Without target	818.777 nA	-98.2541	818.777 nA	-98.2541	818.777 nA	-98.2541
d_t =30mm	39.2547 μA	170.48	24.4068 μA	171.206	3.67716 μA	-177.871
d_t=100mm	5.08511 μA	178.528	3.2154 μA	-175.995	924.466 nA	-128.576
d_t=300mm	818.707 nA	-104.072	817.455 nA	-101.738	817.683 nA	-99.0992

Table 4.10. Receive port induced current of coaxial type coil at d_c = 150 mm in dry soil

d_c=150mm	Sphere(PEC)		Coin(PEC)		Nail(PEC)	
	Magnitude	Phase(deg)	Magnitude	Phase(deg)	Magnitude	Phase(deg)
Without target	622.156 nA	-100.084	622.156 nA	-100.084	622.156 nA	-100.084
d_t =30mm	8.82723 μA	173.325	5.50571 μA	175.722	1.01134 μA	-152.754
d_t=100mm	1.54936 μA	-167.052	1.07826 μA	-155.489	633.967 nA	-111.821
d_t=300mm	622.828 nA	-103.514	622.317 nA	-102.235	622.118 nA	-100.581

Table 4. 11. Receive port induced current of coaxial type coil at d_c = 200 mm in dry soil

d_c=200mm	Sphere(PEC)		Coin(PEC)		Nail(PEC)	
	Magnitude	Phase(deg)	Magnitude	Phase(deg)	Magnitude	Phase(deg)
Without target	432.938 nA	-99.26	432.938 nA	-99.26	432.938 nA	-99.26
d_t =30mm	2.3439 µA	179.921	1.48956 µA	-173.828	479.154 nA	-126.131
d_t=100mm	627.701 nA	-147.14	520.148 nA	-134.419	434.071 nA	-105.122
d_t=300mm	432.82 nA	-101.506	432.797 nA	-101.115	432.941 nA	-99.2323

4.2.3. 8-shaped type coil

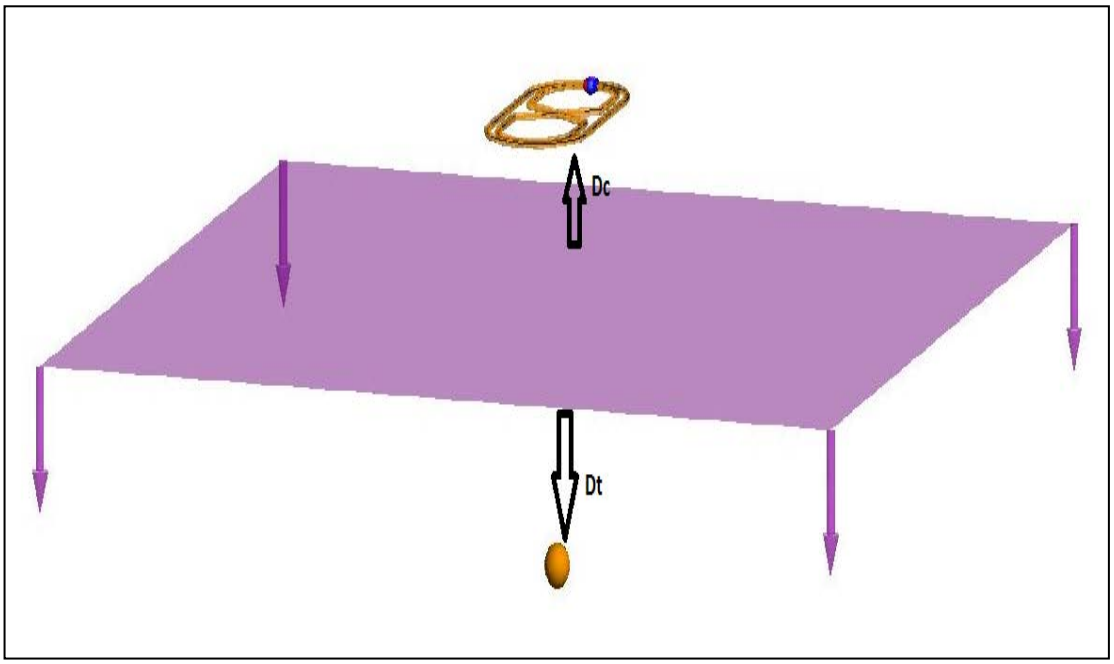

Figure 4. 3. FEKO model of simulation setup with 8-shaped type coil

Table 4. 12. Receive port induced current of 8-shaped type coil at d_c = 50 mm in dry soil

d_c =50mm	Sphere(PEC)		Coin(PEC)		Nail(PEC)	
	Magnitude	Phase(deg)	Magnitude	Phase(deg)	Magnitude	Phase(deg)
Without target	16.5657 mA	-12.6231	16.5657 mA	-12.6231	16.5657 mA	-12.6231
d_t =30mm	16.5508 mA	-12.5882	16.5566 mA	-12.6021	16.5643 mA	-12.6199
d_t =100mm	16.5650 mA	-12.6221	16.5654 mA	-12.6225	16.5653 mA	-12.6229
d_t =300mm	16.5657 mA	-12.6231	16.5657 mA	-12.6231	16.5657 mA	-12.6231

Table 4. 13. Receive port induced current of 8-shaped type coil at d_c = 100 mm in dry soil

d_c =100mm	Sphere(PEC)		Coin(PEC)		Nail(PEC)	
	Magnitude	Phase(deg)	Magnitude	Phase(deg)	Magnitude	Phase(deg)
Without target	16.5657 mA	-12.6231	16.5657 mA	-12.6231	16.5657 mA	-12.6231
d_t =30mm	16.5651 mA	-12.6216	16.5651 mA	-12.6217	16.5655 mA	-12.6228
d_t =100mm	16.5656 mA	-12.6229	16.5656 mA	-12.623	16.5657 mA	-12.6231
d_t =300mm	16.5657 mA	-12.6231	16.5657 mA	-12.6231	16.5657 mA	-12.6231

Table 4. 14. Receive port induced current of 8-shaped type coil at d_c = 150 mm in dry soil

d_c =150mm	Sphere(PEC)		Coin(PEC)		Nail(PEC)	
	Magnitude	Phase(deg)	Magnitude	Phase(deg)	Magnitude	Phase(deg)
Without target	16.5656 mA	-12.623	16.5656 mA	-12.623	16.5656 mA	-12.623
d_t =30mm	16.5654 mA	-12.6227	16.5656 mA	-12.6229	16.5656 mA	-12.623
d_t =100mm	16.5656 mA	-12.623	16.5657 mA	-12.623	16.5656 mA	-12.623
d_t =300mm	16.5656 mA	-12.623	16.5657 mA	-12.623	16.5656 mA	-12.623

Table 4. 15. Receive port induced current of 8-shaped type coil at d_c = 200 mm in dry soil

d_c =200mm	Sphere(PEC)		Coin(PEC)		Nail(PEC)	
	Magnitude	Phase(deg)	Magnitude	Phase(deg)	Magnitude	Phase(deg)
Without target	16.5657 mA	-12.623	16.5657 mA	-12.623	16.5657 mA	-12.623
d_t =30mm	16.5657 mA	-12.6229	16.5657 mA	-12.623	16.5657 mA	-12.623
d_t =100mm	16.5657 mA	-12.623	16.5657 mA	-12.623	16.5657 mA	-12.623
d_t =300mm	16.5657 mA	-12.623	16.5657 mA	-12.623	16.5657 mA	-12.623

Detection of an object by a metal detector strictly depends on electromagnetic properties of soil in which target objects is buried. According to simulation results that have been tabulated above, burying an object beneath dry soil plane changes both magnitude and phase of the receive port induced current too much. For example for DD-type coil, receive port current was 22.2236 mA when there is no target and its phase was around 54°. Then, magnitude of current changes to 12.3046 mA when a soil is placed 500 mm under the center of coil. It is an expected result since soil layer produces a reverse magnetic field and triggers a current on receive coil itself. The amount of magnetic field is directly related to conductivity, relative dielectric permittivity, thermal conductivity, heat capacity, texture of soil, mineralization of soil and magnetic permeability of soil. In this situation, dry soil is a nonmagnetic medium so its μ_r =1 and has a conductivity of 0.01 S/m. This is a relatively big conductivity value and affects the detection drastically so that certain types of soils can reduce the sensitivity of detectors to an extent that they cannot detect targets to desired depths or cause false targets [13]. Also, according to some studies on this subject shows magnetic properties of soil at a certain frequency influences CW metal detectors more than PI detectors since magnetic susceptibility has no frequency dependency [5]. By considering these theoretical approaches and above results, we can conclude that one needs to rebalance its coil by taking into account secondary magnetic field produced by soil itself.

The difference in current magnitude between on air and in dry soil is caused by this secondary magnetic field and since it is too large compared to magnetic field of target, it makes the detection harder and reduces the maximum detection depth independently from coil type. Moreover, results show that with change of d_c, magnitude of current doesn't

change largely in the bad balanced coils (DD-type coil and 8-shaped type coil) but the amount of current changes exceedingly in a well-balanced coil (coaxial type coil) as d_c changes. Another outcome of the results is that again in bad balanced coil types phase of receive current did not change with respect to air results nor to change of d_c. On the other hand, various irregular alterations have been observed in the well balanced coaxial type coil. Advantages and disadvantages of different type these coils are covered in Section 3 and supported with simulation results in Section 4.2. It is observed again in these part of the simulations such as DD-type has a good detection depth again, receive current of coaxial coil decrease dramatically as d_t gets bigger since it suffers from the drawback explained in details in Section 3.4. 8-shaped coil has poor detection sensitivity even though targets were placed at the center of the upper transmit coil independently from the electromagnetic properties of dry soil.

4.3. WET SOIL SIMULATIONS

Third step in our simulation process was simulating all structures in another type of soil which has a greater conductivity than dry soil. We simulate the coils again by locating objects under wet soil at specific depths in this case. Background and analysis of this simulation has already been made in chapter 3. In the following tables simulation results can be seen where d_t represents the distance from surface of ground layer to metallic target and d_c represents the distance from center of coil to surface of ground. Simulation results at for different d_c and d_t values are tabulated in the following four tables.

4.3.1. DD-type coil

Table 4. 16. Receive port induced current of DD-type coil at d_c = 50 mm in wet soil

d_c =50mm	Sphere(PEC)		Coin(PEC)		Nail(PEC)	
	Magnitude	Phase(deg)	Magnitude	Phase(deg)	Magnitude	Phase(deg)
Without target	12.2975 mA	52.659	12.2975 mA	52.659	12.2975 mA	52.659
d_t =30mm	11.7319 mA	52.624	11.7775 mA	52.6195	12.2444 mA	52.6559
d_t =100mm	12.2157 mA	52.6536	12.24 mA	52.655	12.29 mA	52.6585
d_t =300mm	12.2962 mA	52.659	12.2967 mA	52.659	12.2973 mA	52.659

Table 4. 17. Receive port induced current of DD-type coil at d_c = 100 mm in wet soil

d_c =100mm	Sphere(PEC)		Coin(PEC)		Nail(PEC)	
	Magnitude	Phase(deg)	Magnitude	Phase(deg)	Magnitude	Phase(deg)
Without target	12.2961 mA	53.0523	12.2961 mA	53.0523	12.2961 mA	53.0523
d_t =30mm	12.1545 mA	53.0473	12.1927 mA	53.0481	12.2832 mA	53.0519
d_t =100mm	12.2731 mA	53.0516	12.2807 mA	53.0518	12.294 mA	53.0523
d_t =300mm	12.2955 mA	53.0523	12.2957 mA	53.0523	12.2961 mA	53.0523

Table 4. 18. Receive port induced current of DD-type coil at d_c = 150 mm in wet soil

d_c =150mm	Sphere(PEC)		Coin(PEC)		Nail(PEC)	
	Magnitude	Phase(deg)	Magnitude	Phase(deg)	Magnitude	Phase(deg)
Without target	12.2994 mA	53.2604	12.2994 mA	53.2604	12.2994 mA	53.2604
d_t =30mm	12.2619 mA	53.2596	12.274 mA	53.2598	12.296 mA	53.2603
d_t =100mm	12.2917 mA	53.2602	12.2944 mA	53.2603	12.2987 mA	53.2603
d_t =300mm	12.2991 mA	53.2604	12.2993 mA	53.2604	12.2994 mA	53.2604

Table 4. 19. Receive port induced current of DD-type coil at d_c = 200 mm in wet soil

d_c =200mm	Sphere(PEC)		Coin(PEC)		Nail(PEC)	
	Magnitude	Phase(deg)	Magnitude	Phase(deg)	Magnitude	Phase(deg)
Without target	12.2994 mA	53.3805	12.2994 mA	53.3805	12.2994 mA	53.3805
d_t =30mm	12.2877 mA	53.3804	12.2918 mA	53.3805	12.2984 mA	53.3805
d_t =100mm	12.2965 mA	53.3805	12.2975 mA	53.3805	12.2992 mA	53.3805
d_t =300mm	12.2993 mA	53.3806	12.2993 mA	53.3805	12.2994 mA	53.3805

4.3.2. Coaxial type coil

Table 4. 20. Receive port induced current of coaxial type coil at d_c = 50 mm in wet soil

d_c =50mm	Sphere(PEC)		Coin(PEC)		Nail(PEC)	
	Magnitude	Phase(deg)	Magnitude	Phase(deg)	Magnitude	Phase(deg)
Without target	76.9799 nA	160.912	76.9799 nA	160.912	76.9799 nA	160.912
d_t =30mm	170.955 µA	169.294	106.63 µA	169.289	16.1015 µA	169.252
d_t =100mm	21.3639 µA	169.262	13.304 µA	169.243	2.02841 µA	168.974
d_t =300mm	254.33 nA	166.763	187.739 nA	165.865	98.288 nA	162.738

Table 4. 21. Receive port induced current of coaxial type coil at d_c = 100 mm in wet soil

d_c =100mm	Sphere(PEC)		Coin(PEC)		Nail(PEC)	
	Magnitude	Phase(deg)	Magnitude	Phase(deg)	Magnitude	Phase(deg)
Without target	17.5657 nA	-11.5273	17.5657 nA	-11.5273	17.5657 nA	-11.5273
d_t =30mm	39.257 μA	169.293	24.405 μA	169.292	3.59224 μA	169.295
d_t =100mm	5.03519 μA	169.294	3.12158 μA	169.296	449.987 nA	169.323
d_t =300mm	55.4346 nA	169.55	35.2048 nA	169.7	6.74564 nA	-12.8481

Table 4. 22. Receive port induced current of coaxial type coil at d_c = 150 mm in wet soil

d_c =150mm	Sphere(PEC)		Coin(PEC)		Nail(PEC)	
	Magnitude	Phase(deg)	Magnitude	Phase(deg)	Magnitude	Phase(deg)
Without target	113.517 nA	-15.1671	113.517 nA	-15.1671	113.517 nA	-15.1671
d_t =30mm	8.69145 μA	169.349	5.35974 μA	169.385	695.288 nA	170.018
d_t =100mm	1.30648 μA	169.678	771.863 nA	169.946	16.2641 nA	-157.856
d_t =300mm	80.3585 nA	-17.0129	98.4051 nA	-15.8533	110.99 nA	-15.2688

Table 4. 23. Receive port induced current of coaxial type coil at d_c = 200 mm in wet soil

d_c =200mm	Sphere(PEC)		Coin(PEC)		Nail(PEC)	
	Magnitude	Phase(deg)	Magnitude	Phase(deg)	Magnitude	Phase(deg)
Without target	82.5991 nA	165.166	82.5991 nA	165.166	82.5991 nA	165.166
d_t =30mm	2.38604 μA	169.148	1.51127 μA	169.066	285.089 nA	168.097
d_t =100mm	550.374 nA	168.672	368.25 nA	168.366	124.131 nA	166.548
d_t =300mm	97.2952 nA	165.79	85.6783 nA	165.315	83.2269 nA	165.198

4.3.3. 8-shaped type coil

Table 4. 24. Receive port induced current of 8-shaped type coil at d_c = 50 mm in wet soil

d_c =50mm	Sphere(PEC)		Coin(PEC)		Nail(PEC)	
	Magnitude	Phase(deg)	Magnitude	Phase(deg)	Magnitude	Phase(deg)
Without target	16.5655 mA	-12.6237	16.5655 mA	-12.6237	16.5655 mA	-12.6237
d_t =30mm	16.5506 mA	-12.589	16.5564 mA	-12.6029	16.5640 mA	-12.6207
d_t =100mm	16.5652 mA	-12.6231	16.5652 mA	-12.6235	16.5652 mA	-12.6226
d_t =300mm	16.5655 mA	-12.6237	16.5655 mA	-12.6237	16.5655	-12.6237

Table 4. 25. Receive port induced current of 8-shaped type coil at d_c = 100 mm in wet soil

d_c =100mm	Sphere(PEC)		Coin(PEC)		Nail(PEC)	
	Magnitude	Phase(deg)	Magnitude	Phase(deg)	Magnitude	Phase(deg)
Without target	16.5656 mA	-12.6234	16.5656 mA	-12.6234	16.5656 mA	-12.6234
d_t =30mm	16.5647 mA	-12.6211	16.5650 mA	-12.6221	16.5655 mA	-12.6231
d_t =100mm	16.5655 mA	-12.6232	16.5655 mA	-12.6233	16.5656 mA	-12.6233
d_t =300mm	16.5656 mA	-12.6234	16.5656 mA	-12.6234	16.5656 mA	-12.6233

Table 4. 26. Receive port induced current of 8-shaped type coil at d_c =150 mm in wet soil

d_c =150mm	Sphere(PEC)		Coin(PEC)		Nail(PEC)	
	Magnitude	Phase(deg)	Magnitude	Phase(deg)	Magnitude	Phase(deg)
Without target	16.5656 mA	-12.6233	16.5656 mA	-12.6233	16.5656 mA	-12.6233
d_t =30mm	16.5655 mA	-12.623	16.5656 mA	-12.6233	16.5656 mA	-12.6233
d_t =100mm	16.5656 mA	-12.6233	16.5656 mA	-12.6233	16.5656 mA	-12.6233
d_t =300mm	16.5656 mA	-12.6233	16.5656 mA	-12.6233	16.5656 mA	-12.6233

Table 4. 27. Receive port induced current of 8-shaped type coil at d_c = 200 mm in wet soil

d_c =200mm	Sphere(PEC)		Coin(PEC)		Nail(PEC)	
	Magnitude	Phase(deg)	Magnitude	Phase(deg)	Magnitude	Phase(deg)
Without target	16.5656 mA	-12.6232	16.5656 mA	-12.6232	16.5656 mA	-12.6232
d_t =30mm	16.5656 mA	-12.6232	16.5656 mA	-12.6232	16.5656 mA	-12.6232
d_t =100mm	16.5656 mA	-12.6232	16.5656 mA	-12.6232	16.5656 mA	-12.6232
d_t =300mm	16.5656 mA	-12.6232	16.5656 mA	-12.6232	16.5656 mA	-12.6232

Electromagnetic properties of wet soil were tabulated in Table 3.1 and it differs from dry soil having a higher conductivity. So, it was expected again that burying an object beneath wet soil would disrupt any configuration of CW metal detectors since ground plane creates a secondary magnetic field itself. Conductivity of wet soil is approximately 6-7 times greater than conductivity of dry soil in our simulations so a larger change in magnitude and phase of current was expected with respect to air since the reverse magnetic field produced by soil layer will be greater than produced by dry soil. The amount of magnetic field is directly related to conductivity, relative dielectric permittivity but it changed little. During simulations we observed that in order to witness dramatically changes in current, it is necessary to change conductivity to higher values such as 4-5 S/m. This conductivity values nearly correspond to conductivity of sea water. Thus, if we have run these simulations in an extremely conductive media we would see more different results but those environments are not realistic enough to test metal detectors. For example, magnitude of current in DD-type coil simulated in dry soil was 12.3046 mA and 12.2975 mA in wet soil. Although results look like very similar, it has to be noted that our coils have single turn and in case of using multi turn coils it will be easier to see difference between effect of wet soil and effect of dry soil. Phase of the receive port current again did not change largely with respect to dry soil and air in DD-type coil because of same reasons discussed while commenting about results of dry soil simulations.

Just like as in dry soil, reverse magnetic field created by wet soil makes the detection harder and reduces the maximum detection depth independently from coil type. The difference in current magnitude between on air and in wet soil is caused by this secondary

magnetic field and since it is too large compared to magnetic field of target, it makes the detection harder and reduces the maximum detection depth independently from coil type.

Moreover, results show that with change of d_c , magnitude of current does not change largely in coarsely balanced coils (DD-type coil and 8-shaped type coil) but the amount of current changes exceedingly in a well-balanced coil (coaxial type coil) as d_c changes. Another outcome of the results is that again in bad balanced coil types phase of receive current did not change with respect to air results nor to change of d_c. On the other hand, a 180° phase shift has been observed in the well balanced coaxial type coil for some certain d_c values.

4.4. FERROUS SOIL SIMULATIONS

Last step in our simulation process was simulating all structures in a very challenging environment. We simulated our coils in a magnetic soil that has relative magnetic permeability greater than 1 and has same conductivity and relative dielectric permittivity with dry soil. It can be considered as very severe medium that is expected to affect all receive characteristics in receive coil and make the detection process more difficult than other mediums. We called it as ferrous soil by referring its highly magnetic particles. Simulations were performed again by locating objects under wet soil at specific depths in this case. Background and analysis of this simulation has already been made in Section 3. In the following tables simulation results can be seen where d_t represents the distance from surface of ground layer to metallic target and d_c represents the distance from center of coil to surface of ground. Simulation results at for different d_c and d_t values are tabulated in the following four tables.

4.4.1. DD-type coil

Table 4. 28. Receive port induced current of DD-type coil at d_c = 50 mm in ferrous soil

d_c =50mm	Sphere(PEC)		Coin(PEC)		Nail(PEC)	
	Magnitude	Phase(deg)	Magnitude	Phase(deg)	Magnitude	Phase(deg)
Without target	552.904 mA	38.0681	552.904 mA	38.0681	552.904 mA	38.0681
d_t =30mm	552.78 mA	38.072	552.782 mA	38.0699	552.893 mA	38.0865
d_t =100mm	552.886 mA	38.0685	552.891 mA	38.0683	552.901 mA	38.0682
d_t =300mm	552.804 mA	38.0681	552.904 mA	38.0681	552.904 mA	38.0682

Table 4. 29. Receive port induced current of DD-type coil at d_c = 100 mm in ferrous soil

d_c =100mm	Sphere(PEC)		Coin(PEC)		Nail(PEC)	
	Magnitude	Phase(deg)	Magnitude	Phase(deg)	Magnitude	Phase(deg)
Without target	231.897 mA	49.8116	231.897 mA	49.8116	231.897 mA	49.8116
d_t =30mm	231.859 mA	49.8123	231.869 mA	49.812	231.894 mA	49.8117
d_t =100mm	231.891 mA	49.8117	231.893 mA	49.8117	231.897 mA	49.8116
d_t =300mm	231.897 mA	49.8116	231.897	49.8116	231.897 mA	49.8116

Table 4. 30. Receive port induced current of DD-type coil at d_c = 150 mm in ferrous soil

d_c =150mm	Sphere(PEC)		Coin(PEC)		Nail(PEC)	
	Magnitude	Phase(deg)	Magnitude	Phase(deg)	Magnitude	Phase(deg)
Without target	105.121 mA	52.2988	105.121 mA	52.2988	105.121 mA	52.2988
d_t =30mm	105.111 mA	52.299	105.114	52.2989	105.12 mA	52.2988
d_t =100mm	105.119 mA	52.2988	105.12	52.2988	105.121 mA	52.2988
d_t =300mm	105.121 mA	52.2988	105.121	52.2988	105.121 mA	52.2988

Table 4. 31. Receive port induced current of DD-type coil at d_c = 200 mm in ferrous soil

d_c =200mm	Sphere(PEC)		Coin(PEC)		Nail(PEC)	
	Magnitude	Phase(deg)	Magnitude	Phase(deg)	Magnitude	Phase(deg)
Without target	57.7019 mA	53.0572	57.7019 mA	53.0572	57.7019 mA	53.0572
d_t =30mm	57.6986 mA	53.0572	57.6998 mA	53.0572	57.7016 mA	53.0572
d_t =100mm	57.7011 mA	53.0572	57.7014 mA	53.0572	57.7018 mA	53.0572
d_t =300mm	57.7019 mA	53.0572	57.7019 mA	53.0572	57.7019 mA	53.0572

4.4.2. Coaxial type coil

Table 4. 32. Receive port induced current of coaxial type coil at d_c = 50 mm in ferrous soil

d_c =50mm	Sphere(PEC)		Coin(PEC)		Nail(PEC)	
	Magnitude	Phase(deg)	Magnitude	Phase(deg)	Magnitude	Phase(deg)
Without target	202.365 mA	-18.8579	202.365 mA	-18.8579	202.365 mA	-18.8579
d_t =30mm	202.329 mA	-18.8565	202.342 mA	-18.857	202.362 mA	-18.8578
d_t =100mm	202.361 mA	-18.8578	202.362 mA	-18.8578	202.365 mA	-18.8579
d_t =300mm	202.365 mA	-18.8579	202.365 mA	-18.8579	202.365 mA	-18.8579

Table 4. 33. Receive port induced current of coaxial type coil at d_c =100 mm in ferrous soil

d_c =100mm	Sphere(PEC)		Coin(PEC)		Nail(PEC)	
	Magnitude	Phase(deg)	Magnitude	Phase(deg)	Magnitude	Phase(deg)
Without target	47.1018 mA	-13.158	47.1018 mA	-13.158	47.1018 mA	-13.158
d_t =30mm	47.0913 mA	-13.1576	47.0953 mA	-13.1577	47.1009 mA	-13.158
d_t =100mm	47.1005 mA	-13.1579	47.101 mA	-13.158	47.1017 mA	-13.158
d_t =300mm	47.1018 mA	-13.158	47.1018 mA	-13.158	47.1018 mA	-13.158

Table 4. 34. Receive port induced current of coaxial type coil at d_c =150 mm in ferrous soil

d_c =150mm	Sphere(PEC)		Coin(PEC)		Nail(PEC)	
	Magnitude	Phase(deg)	Magnitude	Phase(deg)	Magnitude	Phase(deg)
Without target	14.4019 mA	-11.6657	14.4019 mA	-11.6657	14.4019 mA	-11.6657
d_t =30mm	14.3995 mA	-11.6656	14.4004 mA	-11.6656	14.4017 mA	-11.6657
d_t =100mm	14.4015 mA	-11.6657	14.4017 mA	-11.6657	14.4019 mA	-11.6657
d_t =300mm	14.4019 mA	-11.6657	14.4019 mA	-11.6657	14.4019 mA	-11.6657

Table 4. 35. Receive port induced current of coaxial type coil at d_c = 200 mm in ferrous soil

d_c =200mm	Sphere(PEC)		Coin(PEC)		Nail(PEC)	
	Magnitude	Phase(deg)	Magnitude	Phase(deg)	Magnitude	Phase(deg)
Without target	5.49725 mA	-11.1661	5.49725 mA	-11.1661	5.49725 mA	-11.1661
d_t =30mm	5.4966 mA	-11.1661	5.49685 mA	-11.1661	5.49719 mA	-11.1661
d_t =100mm	5.49712 mA	-11.1661	5.49717 mA	-11.1661	5.49724 mA	-11.1661
d_t =300mm	5.49725 mA	-11.1661	5.49725 mA	-11.1661	5.49725 mA	-11.1661

4.4.3. 8-shaped type coil

Table 4. 36. Receive port induced current of 8-shaped type coil at d_c = 50 mm in ferrous soil

d_c =50mm	Sphere(PEC)		Coin(PEC)		Nail(PEC)	
	Magnitude	Phase(deg)	Magnitude	Phase(deg)	Magnitude	Phase(deg)
Without target	17.7672 mA	-16.343	17.7672 mA	-16.343	17.7672 mA	-16.343
d_t =30mm	17.7666 mA	-16.3412	17.7665 mA	-16.3411	17.7671 mA	-16.3428
d_t =100mm	17.7671 mA	-16.3427	17.7671 mA	-16.3429	17.7672 mA	-16.343
d_t =300mm	17.7672	-16.343	17.7672 mA	-16.343	17.7672 mA	-16.343

Table 4.37. Receive port induced current of 8-shaped type coil at d_c = 100 mm in ferrous soil

d_c =100mm	Sphere(PEC)		Coin(PEC)		Nail(PEC)	
	Magnitude	Phase(deg)	Magnitude	Phase(deg)	Magnitude	Phase(deg)
Without target	16.8141 mA	-13.4058	16.8141 mA	-13.4058	16.8141 mA	-13.4058
d_t =30mm	16.814 mA	-13.4055	16.814 mA	-13.4057	16.8141 mA	-13.4058
d_t =100mm	16.8141 mA	-13.4058	16.8141 mA	-13.4058	16.8141 mA	-13.4058
d_t =300mm	16.8141 mA	-13.4058	16.8141 mA	-13.4058	16.8141 mA	-13.4058

Table 4. 38. Receive port induced current of 8-shaped type coil at d_c =150 mm in ferrous soil

d_c =150mm	Sphere(PEC)		Coin(PEC)		Nail(PEC)	
	Magnitude	Phase(deg)	Magnitude	Phase(deg)	Magnitude	Phase(deg)
Without target	16.6512 mA	-12.8946	16.6512 mA	-12.8946	16.6512 mA	-12.8946
d_t =30mm	16.6511 mA	-12.8945	16.6511 mA	-12.8945	16.6512 mA	-12.8946
d_t =100mm	16.6512 mA	-12.8946	16.6512 mA	-12.8946	16.6512 mA	-12.8946
d_t =300mm	16.6512 mA	-12.8946	16.6512 mA	-12.8946	16.6512 mA	-12.8946

Table 4. 39. Receive port induced current of 8-shaped type coil at d_c = 200 mm in ferrous soil

d_c =200mm	Sphere(PEC)		Coin(PEC)		Nail(PEC)	
	Magnitude	Phase(deg)	Magnitude	Phase(deg)	Magnitude	Phase(deg)
Without target	16.6041 mA	-12.7454	16.6041 mA	-12.7454	16.6041 mA	-12.7454
d_t =30mm	16.6041 mA	-12.7454	16.6041 mA	-12.7454	16.6041 mA	-12.7454
d_t =100mm	16.6041 mA	-12.7454	16.6041 mA	-12.7454	16.6041 mA	-12.7454
d_t =300mm	16.6041 mA	-12.7454	16.6041 mA	-12.7454	16.6041 mA	-12.7454

Ferrous soil was defined as a magnetic medium and its electromagnetic properties were tabulated in Table 3.1. Ferrous soil is considered as the most challenging medium for operation of metal detectors since the dominant parameter in the occurrence of reverse magnetic field is magnetic susceptibility, not conductivity nor dielectric permittivity. The electrical conductivity plays a secondary role expected to have a significant effect for highly conducting soils only [6]. We can see that from above results that although ferrous soil has been defined with the same conductivity of dry soil, it behaves completely different than dry soil. Our ferrous soil media has a magnetic permeability 12 and this value is large enough to define it as a severe media. A severe media is an environment in which coil detection is primarily effected by soil conditions as it can be seen on simulation results. Since ferrous soil has very high iron content, it can cause number of false alarms

easily and reduce the sensitivity of MD. In order to overcome this problem, a detector has to be highly ground balanced.

When ferrous soil is placed 50 mm under coil center, current of receive coil has been boosted from 20.2236 mA to 552.904 mA with respect to on air condition in DD-type coil when there is no target. A great change also has been observed in induced current of coaxial type coil in ferrous soil as expected. On the other hand phase of current does not change with increasing d_t or d_c. An interesting result for coaxial type coil is that although it was the best balanced coil and showed better performance in other types of soils, in ferrous soil it loses its pretty satisfying balance and has a receive port current more than 1000 times bigger compared to current in dry soil or wet soil resulting loss in detection depth and erratic responses. These results shows that in highly mineralized soils even a well-balanced coil exhibits poor performance and cause to false alarms and in these types of soil a careful ground balancing is strictly necessary to get an acceptable performance. Ground balancing operation is basically a function of adjusting the metal detector to ignore the unwanted effect of specific minerals in the soil so that they are not detected by the metal detector.

4.5. MATLAB ANALYSIS

In addition to the FEKO analysis of proposed coil structures, a basic signal analysis was performed on MATLAB. As it was specified in the previous sections of this thesis, in FEKO, transmit coil was fed by a continuous wave signal since we could not excite coil with a pulse signal. In this section, a pulse train is defined in MATLAB as the excitation signal and this pulse train is convolved with the time domain equivalent of induced port current signal that is obtained in FEKO in order to see how coil would behave with a pulse excitation. Illustration of the pulse can be seen in the following figure and also its parameters are tabulated in Table 4.40.

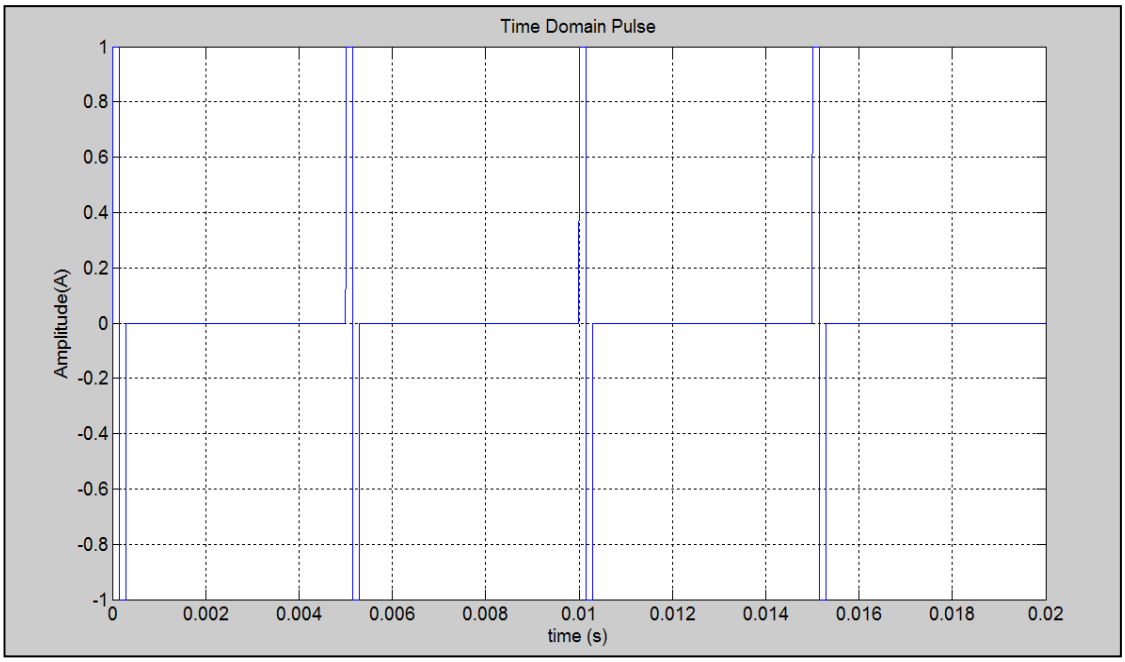

Figure 4.4. Pulse excitation signal

Table 4.40. Parameters of pulse

Amplitude	1 V_p
Rise time	5 μs
Hold time	140 μs
Fall time	5 μs

In FEKO, a new simulation set was performed for only DD-type coil on air without target condition at 100 KHz. Induced current on the receive port in the frequency domain for this set of simulation is in Figure 4.5.

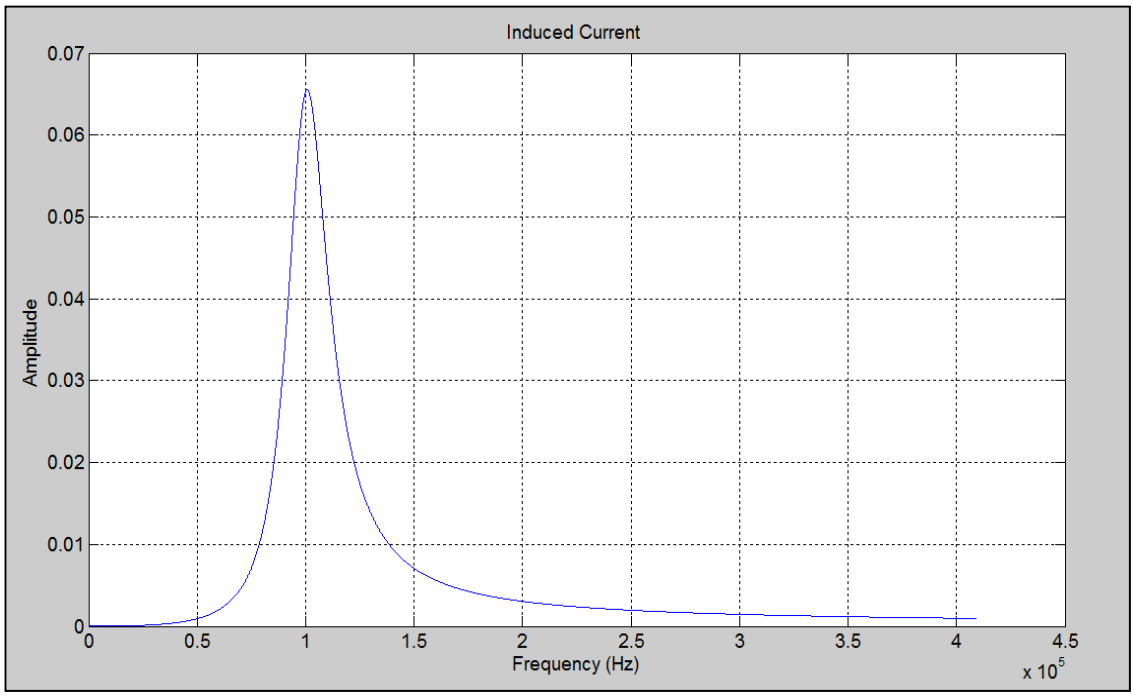

Figure 4.5. Induced current in receive coil imported from FEKO simulation

Then, Inverse Fast Fourier Transform (IFFT) was applied to the above frequency domain signal to represent it in time domain.

At the end, time domain excitation pulse signal and IFFT of the induced current was convolved to see the characteristics of specified coil in time domain. Result of this convolution process is presented in the below figure.

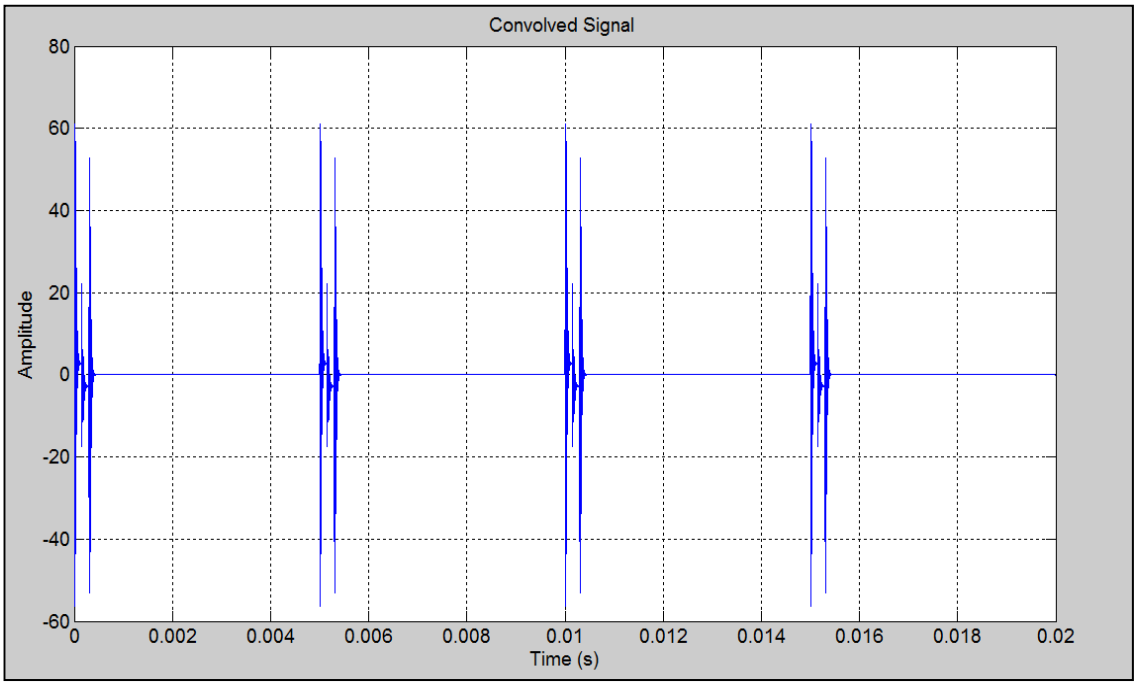

Figure 4.6. Convolved Signal

5. REALIZATION AND MEASUREMENTS

After performing simulations for all types of coil geometries, we have selected coaxial type coil to construct and make some measurements with it. These measurements have been performed to see how it works and to compare measurement results with the simulation results. Coaxial type coil is selected since it had the best performance in terms of detection capabilities and also easy to obtain nearly perfect induction balance even if it is constructed with simple wounding techniques. The same coil structure which is investigated in details in Section 3.3 with two receive coils and one transmit coil is used in measurements.

In the simulations both receive and transmit coils had only one turn to achieve simplicity and reduce simulation time. However, 15 turns are used in both receive and transmit coils when we were realizing them in order or be able to increase the amount of induction current. This increase in the induction current allowed us to detect this current in the oscilloscope properly. As it is explained in Section 2 of this thesis, using a coil with 15 turns increases the induction current 225 times. However, this increment in the receive port induction current will not be sufficient to detect it with the oscilloscope. To overcome this problem, a very simple non-inverting amplifier circuit is used that has a maximum gain around 16 at our operating frequency limited by gain-bandwidth product of the opamp. Amplifier circuit is designed with LM741 general purpose OpAmp and specific resistor values to get a gain 16 at operating frequency. Circuit is fed by +15V, -15V DC source as specified in the datasheet. The amplifier circuit is shown in Figure 5.1.

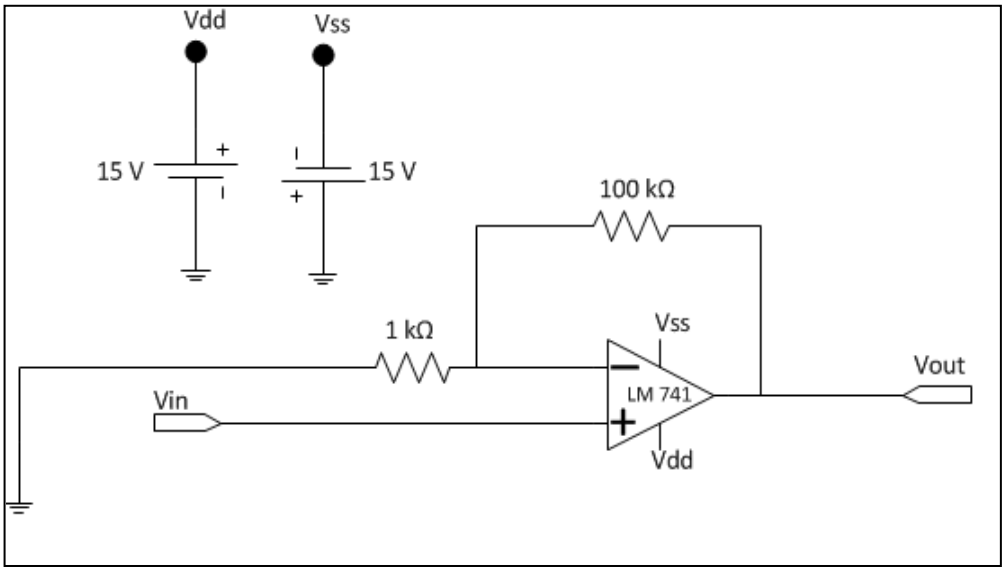

Figure 5.1. Amplification circuit

After applying this amplification to receive port current, it finally became possible to see difference between current values as metallic target moves along the vertical axis of the coil on air. Picture of the constructed coaxial type coil can be seen in Figure 5.2.

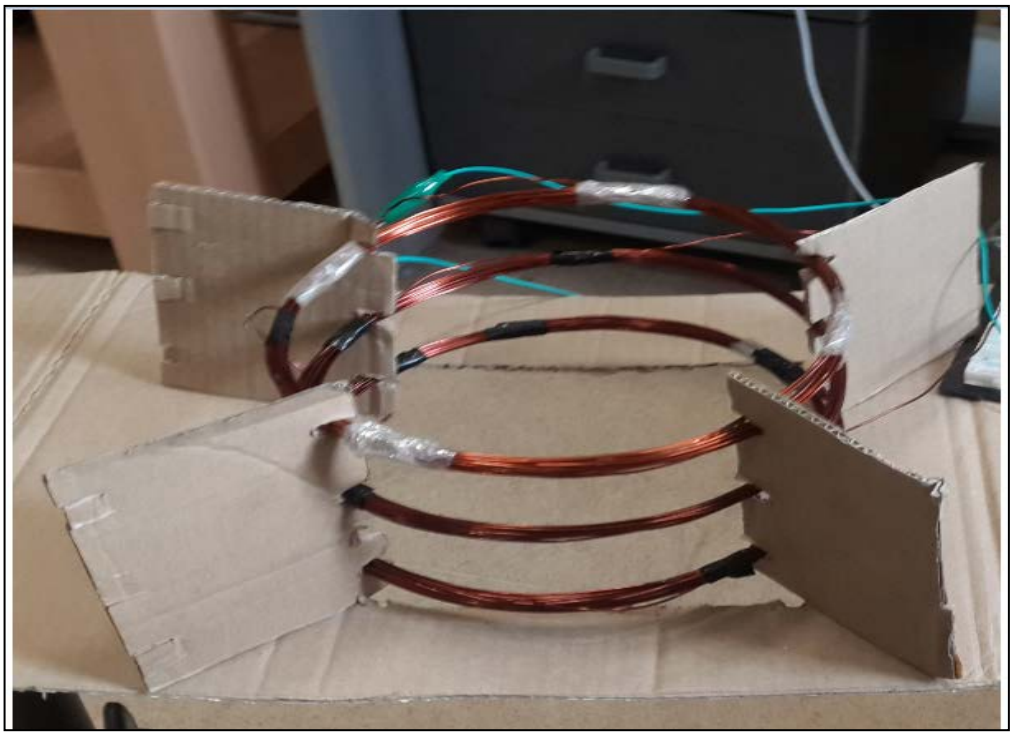

Figure 5.2. Constructed coaxial type coil with 15 turns

In the coil, enameled copper wire that has a 1.2 mm diameter is used. After winding receive coil, its inductance was measured with a LRC meter and it was found as approximately 205 μH. This value is consistent by comparing the inductance value of one turn coil that is calculated by simulation. Then, same calculation is performed as in Section 3 to find the capacitance values that will make the coil resonant at 150 kHz as follows.

$$L = 205\ x\ 10^{-6}\ H$$

From the resonance formula,

$$f = \frac{1}{2\ \pi\ \sqrt{L\ C}}$$

$$150\ x\ 10^{3} = \frac{1}{2\ \pi\ \sqrt{205\ x\ 10^{-6}.\ C}}$$

So, necessary capacitance value becomes,

$$C = 5.63\ x\ 10^{-9}\ F$$

Coil is made resonant by using discrete a discrete capacitor set that has a value approximately 5.6 nF. Also, measured value of coil resistance is about 1.1 Ω.

During measurements, a 1 $V_{p\text{-}p}$ sine signal is applied at 150 kHz via a signal generator. Receive coil induction current is observed in the oscilloscope after passing an amplifier circuit that is mentioned above. The measurement setup is shown in Figure 5.3.

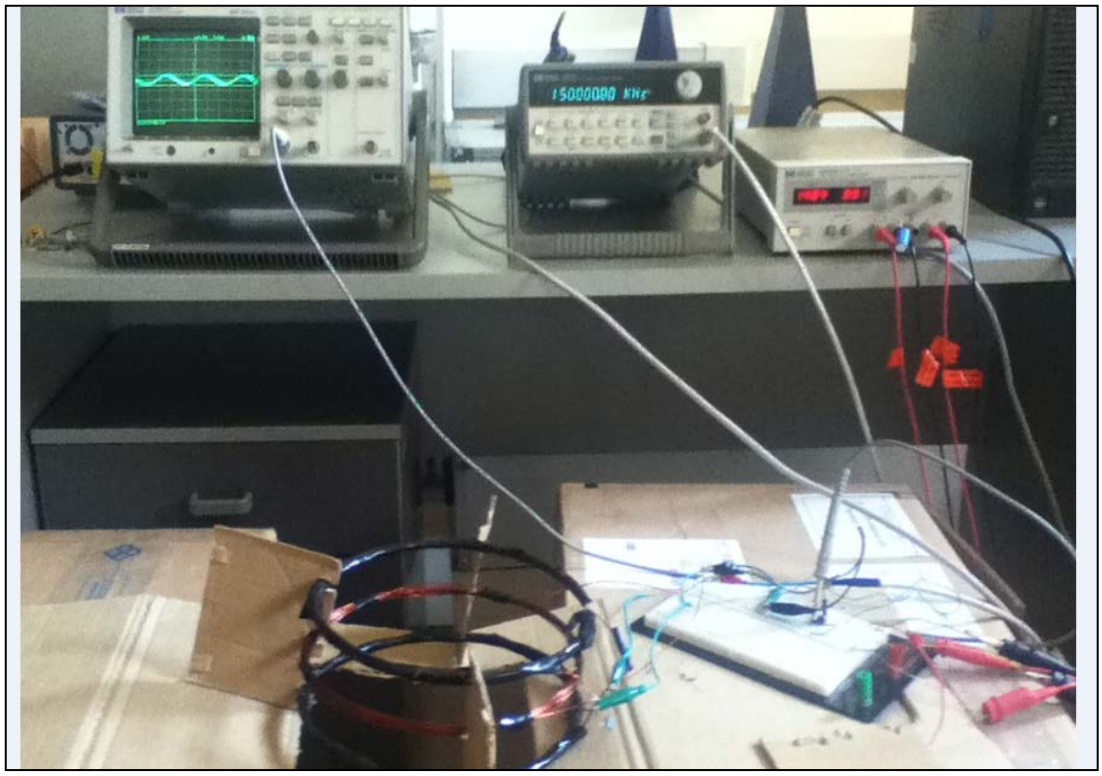

Figure 5.3. Measurement setup for coaxial type coil

In the measurements, three types of metallic targets were used as in the simulations. A coin that has a 20 mm radius and 10 mm height and a nail that has 50 mm length are used. But, instead of a spherical metallic target a metallic cube is used since it was easier to make by hand compared to sphere. Sphere was the target that has the largest surface and so easiest to detect according to simulation results. By considering this, in order to replace sphere with a corresponding object, edge length of the cube is selected as 30 mm to give maximum surface among three objects just like in the simulations. All targets were made from copper. Images of these three metallic targets can be seen in Figures 5.4, 5.5 and 5.6 respectively.

Figure 5.4. Coin target

Figure 5.5 Nail target

Figure 5.6 Cubic target

Measurements were performed with above three metallic targets at different depths along vertical axis of the coil. Value of receive port induced voltage can be found for three different targets for different depths can be found in the following tables. All measurements were performed for on air condition. Note that the oscilloscope that we use during measurements was not precise enough to measure and show the exact changes in the induced voltage as target moves along axis. So, only least significant figures of the following results may be imprecise. Results are tabulated in the form of voltage where d_t represents the vertical distance between center of coil and the location of metallic target.

In this point also simulations for cubic target was performed in FEKO for only coaxial type coil on air condition in order to be able to make meaningful comparisons between simulated and measured cases.

Table 5.1. Induced voltage in the receive coil

	Cube(Copper) m	Coin(Copper)	Nail(Copper)
Without target	118.1 mV	118.1 mV	118.1 mV
d_t =50mm	503.1 mV	243.1 mV	162.1 mV
d_t =100mm	318.1 mV	193.1 mV	139.1 mV
d_t =150mm	213.1 mV	169.1 mV	130.1 mV
d_t =200mm	146.1 mV	140.1 mV	127.1 mV
d_t =250mm	137.1 mV	130.1 mV	124.1 mV
d_t =300mm	131.1 mV	126.1 mV	121.1 mV
d_t =400mm	128.1 mV	121.1 mV	118.1 mV
d_t =500mm	124.1 mV	120.1 mV	118.1 mV

Simulated values of coin, nail and cube target and their measured values are drawn as pairs in terms of receive port induced currents and can be seen in the following figures to investigate the relationship between simulations and measurements. Here, it has to be noted that measured values are induced voltages and also they are increased 16 times by an amplifier circuit and 225 times by turn ratios. So, to make reasonable comparisons, measured values were normalized to one turn, non-amplified induced current values.

Moreover, while comparing these measurement results with the simulation results, it should be considered that in the simulations all targets were constructed from PEC, but in measurement case they were made from copper that causes a certain AC resistance during current flow. Moreover, in simulations all of the conditions were ideal but in measurements there were some uncontrollable parameters and irregularities such as sensitivity of oscilloscope as it is mentioned before, existence of other unintentionally placed metallic objects in the proximity of coil, difference in the diameter of coil wires etc.

Thus, observing the exactly same amount of induced current in simulation and measurements was something difficult and unexpected in our case. What we want to see was observing the same behavior of coil in the measurements with respect to simulations in terms of amount of change in the induced current as target closes to coil, increment in the induced current as surface area of target increases, how deep coaxial coil can detect targets etc. Nevertheless, it was also observed relatively close relationship in the values of

simulated and measured induced current when we normalize the measured current voltage value especially for depths between 100 mm and 250 mm. Since there already was an induced voltage around 120 mV when there is no target in the measurements, difference in the induced current cannot be observed as clear as in the simulations beyond 300 mm depth. An unavoidable erroneous measurement of oscilloscope around 15 mV and amplification of this factor by amplifier circuit caused this sensitivity weakness for specified depths for all types of targets.

For example, if coin target is investigated when it is placed at 150 mm under the center of coil, its simulated induced current value is around 21 μA according to Table 4.2. And its measured induced voltage value is about 213 mV. To switch to current parameter, AC resistance of constructed receive coil can be calculated by using the below formulas.

$$R_{ac} = \frac{\rho \, x \, l}{A_{eff}} \tag{5.1}$$

$$A_{eff} = \delta \, x \, \pi \, x \, d \tag{5.2}$$

$$\delta = \sqrt{\frac{\rho}{\pi \, xf \, x\mu}} \tag{5.3}$$

Where,

- ρ represents the resistivity of material,
- l represents length of coil
- A_{eff} represents effective cross sectional area
- d represents diameter of wire used in coil
- f represents operating frequency
- δ represents skin depth.

If calculations are performed with our parameters AC resistance of realized receive coil it is found as approximately 0.57 Ω. So, by dividing induced voltage value, 213 mV to this

resistance induced voltage can be found as 373 mA. To normalize this current, it has to be divided by 16 to remove amplifying effect and then by 225 to remove the increment comes from turn ratios. After these operations normalized measured induced current at the receive coil can be found as nearly 16 μA which is very close to 21 μA simulated in FEKO.

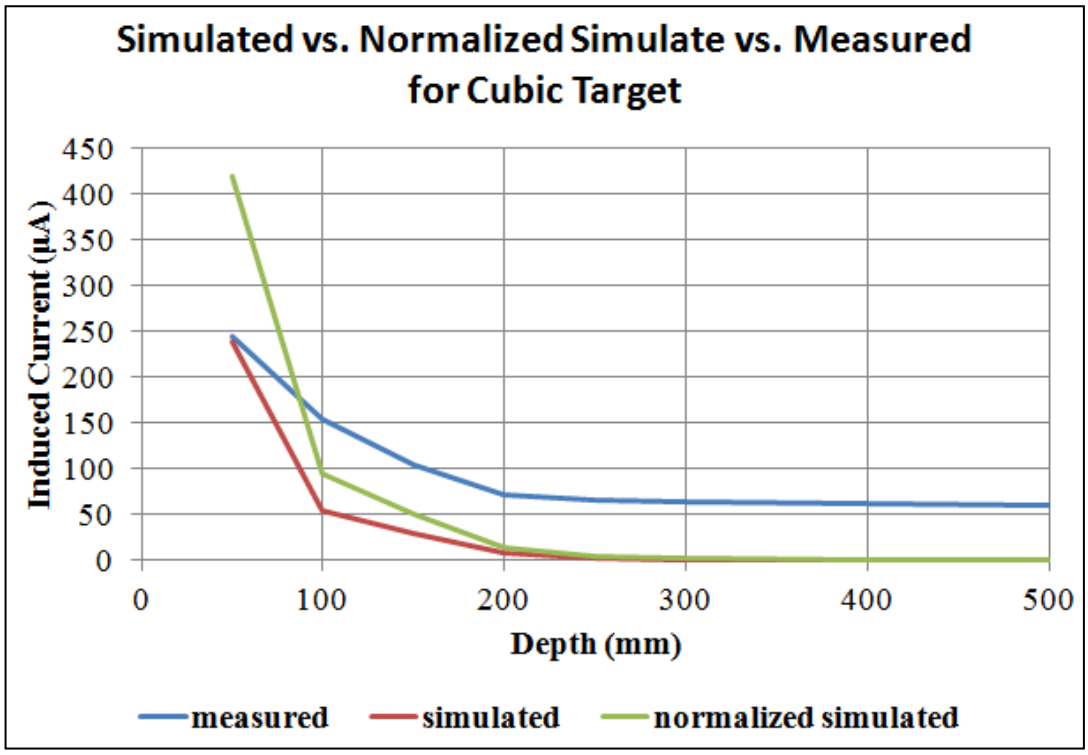

Figure 5.7. Simulated vs. measured results for cubic target

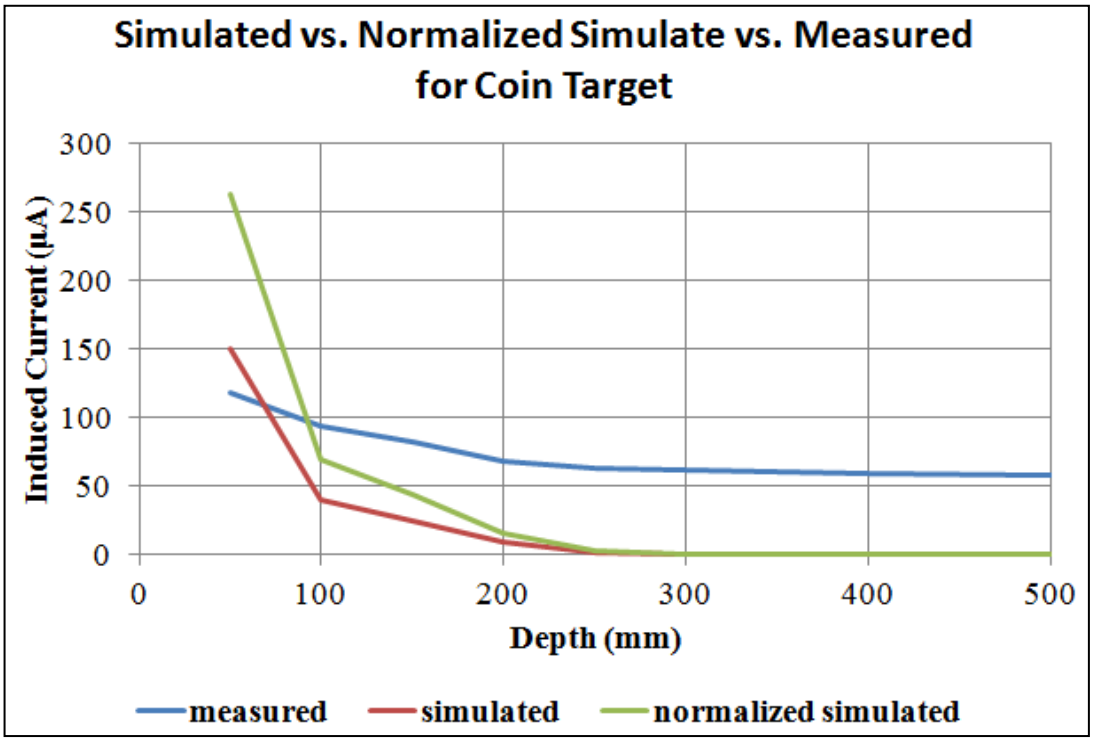

Figure 5.8. Simulated vs. measured results for coin

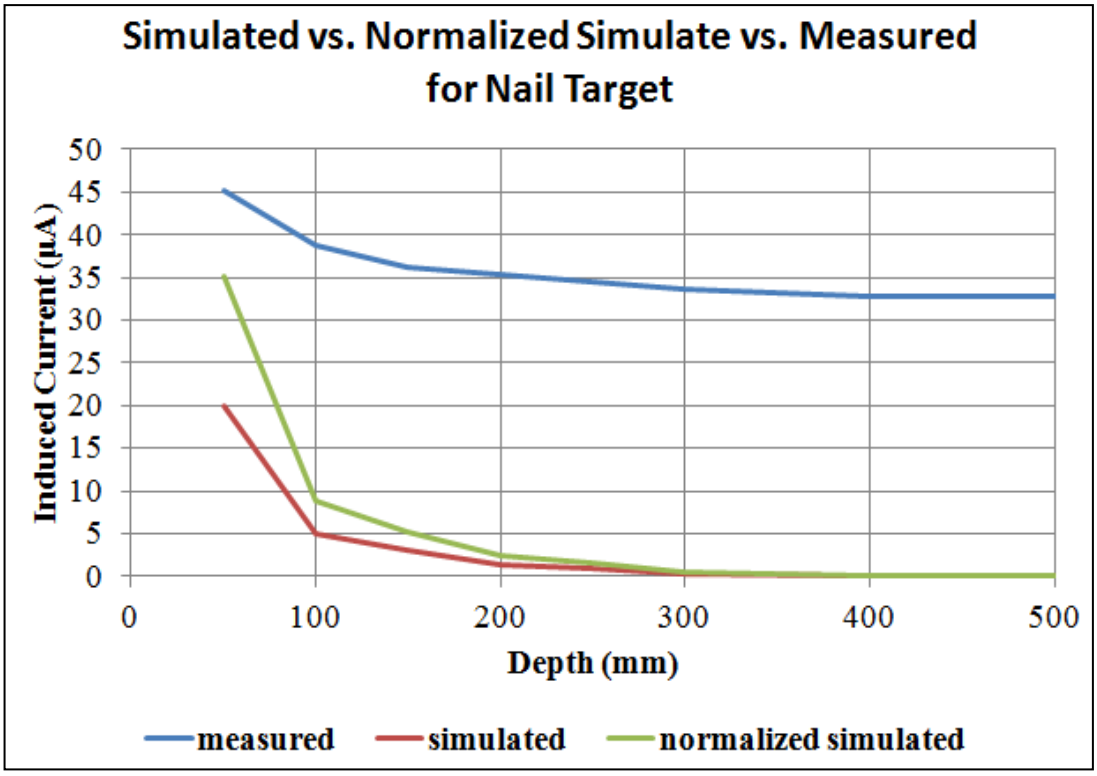

Figure 5.9. Simulated vs. measured results for nail

Also, as it can be seen from measurement results, detection capability of measured coil diminishes with increasing depth but decrement in the receive port difference occurs very fast just like in simulations. Magnitude of current decreases dramatically as d_t gets larger. Again as observed in the simulations, measured coil can detect targets that have greater surface area more easily than others. According to measurement results cube is the easiest one to detect since it has the greatest surface area whereas nail is a very challenging object and coil cannot detect it for the depths greater than 350 mm.

6. CONCLUSION

In this study, three different coil geometries were studied and optimized to use in low frequency electromagnetic induction sensors at 150 kHz. Simulations and optimization process were performed in FEKO. Detection performance of DD type coil, coaxial type coil and 8 shaped type coil were investigated in detail. All coil types were optimized on air and then simulated to observe detection characteristics in more realistic soil types.

According to simulation results, coaxial type coil was the most successful coil among others by providing a much better induction balance in the receive coil(s). However, major drawback of coaxial type coil that its limited and relatively small detection depth because as depth gets larger significant amount of signal cancellation occurs between two "+" polarized coil and "-" polarized coil.

DD type coil was also studied and it was shown that it exhibited poor induction balance performance compared to coaxial type coil. But, this type of coil offers a deeper but narrower detection area than other types. However, its performance and reliability was not as good as coaxial type coil in detecting small nail target at the same depth in close proximity of the search head.

8 shaped type coil was the coil that shows the poorest detection performance since the magnetic field created by transmit coil has a null at the crossover. This disadvantage caused very poor detection sensitivity at the main axes of the search head along where our targets were located.

After optimizing and evaluating the coil geometries in free space, effects of dry soil, wet soil and ferrous soil were investigated. First, dry soil was simulated and a decrement in the detection capability with respect to depth was observed because dry soil is a conductive media and produces a reverse magnetic field and triggers a current on receive coil itself. Moreover, simulation results show that with change of d_c, magnitude of current does not change largely in the bad balanced coils (DD-type coil and 8-shaped type coil) but the

amount of current changes considerably in a well-balanced coil (coaxial type coil) as d_c changes.

Wet soil is studied next and electromagnetic properties of wet soil differs from dry soil with 6-7 times great conductivity value. It is observed that relatively large changes occur in magnitude and phase of receive port induced current with respect to dry soil since the amount of reverse magnetic field produced by soil is directly related to conductivity of media.

Finally, a challenging environment for metal detectors, ferrous soil was studied. Although ferrous soil was defined with the same conductivity of dry soil, reverse magnetic field and adverse effects of ferrous soil were greater than other soil types since dominant parameter in the occurrence of reverse magnetic field is magnetic susceptibility, not conductivity nor dielectric permittivity. Better induction balance is necessary for metal search heads that are intended to be used in ferrous environments.

Additionally, induced voltage measurements were performed for coaxial type coil in air and reasonable corroboration between simulation and measurement results was observed in terms of detection characteristics.

REFERENCES

1. Druyts, P., *Analysis of Environmental Effects on Electromagnetic Induction Sensors*, Ph.D Thesis, Louvain School of Engineering, 2011.

2. Bruschini, C., *A multidisciplinary Analysis of Frequency Domain Metal Detectors for Humanitarian Demining*, Ph.D Thesis, Vrije University, 2002.

3. Svatoš, J., Nováček, P. and Vedral, J., "sin(x)/x Signal Utilization in Metal Detection and Discrimination", *Journal of Electrical Engineering*, Vol. 63, No 7s, pp. 110-113, 2012.

4. Das, Y. and Toews, J.D., "Issues in Performance Evaluation of Metal Detectors", *Canadian Centre for Mine Action Technologies*, pp.1-17, 1996.

5. Cross, G., "Soil Electromagnetic Properties and Metal Detector Performance: Theory and Measurement", *Canadian Centre for Mine Action Technologies*, 2008.

6. Druyts, P., Yvinec, Y. and Acheroy, M., "A Framework to Relate Soil Properties to Soil Classes Based on Performance of Metal Detectors and Dual Sensors", Royal military School of Belgium, 2011.

7. Van D., Renke L., Borchers, B. and Hendricks, J.M.H., "Strength of Landmine Signatures Under Different Soil Conditions: Implications for Sensor Fusion", *Int J. Systems Science* Vol. 36, pp. 573-588, 2005.

8. Guelle, D., Smith, A., Lewis, A. and Bloodworth, T., *Metal Detector Handbook* Luxembourg, 2003.

9. Lewis, A.M., Verlinde, P., Peichl, M., Ebert, R. and Klein, V., Multisensor Mine Signatures Report, *ITEP Project 2.5.1.2*, 2004.

10. Reuter, M., Tadjine, H.H., Harneit, S., “Localisation and Detection of Buried Objects like Mines in Diverse Soils with Soft Computing Methods”, *The European Conference on Non-Destructive Testing*, 2006.

11. Yesil, M. A., Yegin, K., Bellikli, H., Tura, L., Nazli, H. and Dag, M., “Multi-channel transmit/receive metal detector coil design for vehicular applications”, *Proc. SPIE 9072, Detection and Sensing of Mines, Explosive Objects, and Obscured Targets XIX*, 2014.

12. Moreland, C., “Coil Basics”, *Geotech*, 2006.

13. Das, Y., “A Preliminary Investigation of the Effects of Soil Electromagnetic Properties on Metal Detectors”, *Proc. SPIE 5415, Detection and Remediation Technologies for Mines and Minelike Targets IX*, 2004.

14. Moreland, C.W., “BFO Theory”, *Geotech*, 1999.

15. Wessels, C. and Palag, T., Construction of a Beat Frequency Oscillator Metal Detector, *Electrical and Computer Engineering University of Colorado*, 2009.